Bachelor's Thesis in Microsystems Engineering

Development of an LED Array for Optogenetic Long-Term Stimulation of Neuronal Networks in Vitro

Nicolas Christoph Steenbergen

Supervisors: Dr. Samora Okujeni,
Prof. Dr. Ulrich Egert

Albert-Ludwigs-University Freiburg

Faculty of Engineering

Biomicrotechnology, Dept. of Microsystems Engineering

IMTEK

January 31st, 2023

Writing Period

31.10.2022 – 31.01.2023

Supervisors

Dr. Samora Okujeni and Prof. Dr. Ulrich Egert

Technical assistance

Ute Boltze

Declaration

I hereby declare, that I am the sole author and composer of my thesis and that no other sources or learning aids, other than those listed, have been used. Furthermore, I declare that I have acknowledged the work of others by providing detailed references of said work.

I also hereby declare that my thesis has not been prepared for another examination or assignment, either in its entirety or excerpts thereof.

Titisee-Neustadt, 31.01.2023

Place, Date

Signature

Abstract

In this work, the development of a platform for long-term optogenetic stimulation of neuronal networks in vitro is described. The aim of this platform is to investigate the effects long-term optogenetic stimulation has on neurons during homeostatic, activity-dependent network development.

The subjects of stimulation are networks of around $2 \cdot 10^5$ neurons, which are to be cultivated on standardized 12-well cell carrier substrates. Each culture (one per well) of the carrier should be continuously stimulated by one LED and not be affected by other LEDs in the array. Different LED pulse timings and frequencies should be possible. Additionally, the stimulation must be carried out under predefined incubator conditions (95 % humidity and 37 °C) and must not significantly increase the temperature in the local microenvironment of developing cultures.

The first part of this work describes the development of the platform, from its functional requirements to the construction, programming and realization of two prototypes. The second part of this work discusses an experiment conducted with both prototypes as well as experiments conducted with a micro-electrode array (MEA). The purpose of the MEA experiment was to assess the effectiveness of optogenetic stimulation in dependence of the distance between LED and neuronal network. The electrophysiological, optogenetic and microanatomic processes and analysis methods used in this work are described. Similarly, the morphological effects of long-term stimulation with the platform on developing neuronal networks are discussed.

Zusammenfassung

In dieser Arbeit wird die Entwicklung einer Plattform zur optogenetischen Stimulation neuronaler Netzwerke in vitro beschrieben. Ziel dieser Plattform ist es, die Auswirkungen zu untersuchen, die langfristige optogenetische Stimulation auf Neuronen während der homöostatischen, aktivitätsabhängigen Netzwerkentwicklung haben.

Gegenstand der Stimulation sind Netzwerke von etwa $2 \cdot 10^5$ Neuronen, die auf standardisierten 12-Well-Zellkulturplatten kultiviert werden sollen. Jede Zellkultur (eine pro Senke) der Zellkulturplatte sollte von einer LED für eine kontinuierliche Stimulation beleuchtet werden und nicht durch andere LEDs im Array beeinflusst werden. Verschiedene LED-Pulszeiten und -frequenzen sollten möglich sein. Außerdem muss die Stimulation unter vordefinierten Inkubationsbedingungen (95 % Luftfeuchtigkeit und 37 °C) erfolgen und darf die Temperatur in der Mikroumgebung der sich entwickelnden neuronalen Zellkultur nicht signifikant erhöhen.

Im ersten Teil dieser Arbeit wird die Entwicklung der Plattform beschrieben, von den funktionalen Anforderungen bis hin zur Konstruktion, Programmierung und Realisierung von zwei Prototypen. Der zweite Teil dieser Arbeit beschreibt ein Experiment, das mit beiden Prototypen durchgeführt wurde, sowie Experimente, die mit einem Multi-Elektroden-Array (MEA) durchgeführt wurden. Der Zweck des MEA-Experimentes war es, die Wirksamkeit optogenetischer Stimulation in Abhängigkeit des Abstandes zwischen LED und neuronaler Zellkultur zu ermitteln. Die in dieser Studie eingesetzte elektrophysiologische, optogenetische und mikroanatomische Verfahren und Analysemethoden werden beschrieben. Ebenso werden die morphologischen Auswirkungen der Langzeitstimulation mit der Plattform auf die sich entwickelnden neuronalen Netze erörtert.

Table of Contents

Abstract III

Zusammenfassung V

Table of Contents VII

Table of Figures X

Table of Abbreviations and Acronyms XII

Culture Identifiers XIII

1 Introduction 2

1.1 Optogenetic Interference with Homeostatic Network Development in vitro 2

1.2 Optogenetics Explained 4

1.3 Scientific Objective 5

1.3.1 Functional Requirements 5

2 Materials & Methods 9

2.1 Technical Documentation 9

2.1.1 LED 9

2.1.2 Circuitry 11

2.1.3 Microcontroller 11

2.1.4 Construction 11

2.1.5 Second Prototype 12

2.1.6 Programming 13

2.2 LTS Experiment Documentation 15

2.2.1 Overview 15

2.2.2 Timeline 16

2.2.3 Immunohistology & Microscopy 16

2.2.4 Analysis 17

2.3 MEA Experiment Documentation 18

3 Results 20

3.1 LED Stimulation Platform for Optogenetic LTS 20
3.2 MEA Experiment Results 20
3.3 LTS Experiment Results 23
3.3.1 Densities 24
3.3.2 Clustering Index 24
3.3.3 Axon length 25
4 Discussion 33
4.1 Prototype Review 33
4.2 Explanatory Models for LTS Experiment Results 34
4.2.1 Impact of LTS on Cell Survival 34
4.2.2 Impact of LTS on neuronal migration 36
4.2.3 Impact of LTS on axon growth 37
4.2.4 Summary of Findings 37
4.3 Effectiveness of Optogenetic Stimulation 37
4.4 Relevance of Results 38
5 Summary 40
6 Acknowledgments 42
7 Bibliography 45

Table of Figures

Figure Number	Description	Page Number
1	Evolution of network spikes	3
2	Neuronal activity profiles	3
3	Stimulation pattern	7
4	Example of matrix multiplexing	7
5	Geometry of a spherical cone	9
6	Matrix multiplexing circuit diagram	10
7	Directly connected circuit diagram	10
8	12-well cell culture carrier	10
9	Early stimulator prototype	10
10	Side-on view of the stimulator	10
11	Second prototype construction	14
12	Stimulator circuits	14
13	Completed stimulators	15
14	LTS experiment timeline	15
15	MEA experiments documentation	18
16	PSTH array	21
17	Selected PSTHs and spiking activity	22
18	Network burst waveform	23
19	Photoelectric effect waveform	23

20	Micrograph grid	26
21	Micrograph close-up of CC2 B3	27
22	CC1 morphological analysis	28
23	CC1 normalized morphological analysis	29
24	CC2 morphological analysis	30
25	CC2 normalized morphological analysis	31

Table of Abbreviations and Acronyms

MEA	Micro-Electrode Array
AP	Action Potential
CI	Clustering Index
ChR2	Channelrhodopsin 2
DIV	Day(s) In Vitro
GND	Ground
GPIO	General-Purpose Input/Output
LED	Light Emitting Diode
LTS	Long-Term Stimulation
S1	First Stimulator
S2	Second Stimulator
PSTH	Peristimulus Time Histogram
WIV	Week(s) In Vitro
UV	Ultraviolet

Culture Identifiers

Name	Abbreviation	Identifier
Cell Culture 1	CC1	PID509 CID7670
Cell Culture 2	CC2	PID509 CID7668
Cell Culture 3	CC3	PID508 CID7656
Cell Culture 4	CC4	PID509 CID7654
Cell Culture 5	CC5	PID509 CID7665

1 Introduction

1.1 Optogenetic Interference with Homeostatic Network Development in vitro

Cultured neurons form electrically active networks during development and undergo a similar maturation process as neurons developing in vivo (Okujeni and Egert 2019; Ramakers et al. 1990). During their early growth, neurons migrate and elaborate their axons and dendrites, connecting to one another to form synapses. Herein, neuronal migration and neurite outgrowth are regulated by neuronal activity-related Ca^{+} influx. Such influx act on cytoskeletal dynamics via complex biochemical pathways (Lambert de Rouvroit and Goffinet 2001). Optogenetic stimulation of neurons via channelrhodopsins induce indirect or direct increases in Ca^{2+} influx (Nagel et al. 2002). This suggests possible means to shape the structure and connectivity of developing neuronal networks by influencing with the morphological differentiation process (Lignani et al. 2013). However, the interactions between chronic stimulation and homeostatic network growth are currently poorly understood.

In this work, we developed a platform for the optogenetic stimulation of developing neuronal networks and analyzed the morphological effects of long-term optogenetic stimulation. Current models of neuronal activity-dependent outgrowth and migration suggest that during development, neurons regulate their interconnectivity to reach a homeostatic set point of activity and Ca^{+} influx (Okujeni and Egert 2019; van Ooyen et al. 1995). Neuronal activity emerges spontaneously by the end of the first week in vitro (WIV). Stable levels of activity are reached in the fourth WIV (van Pelt et al. 2005). When neurons spontaneously fire such action potentials (AP), these signals are transmitted between neurons via synapses, the connections between neurons. Such synaptic transmission excites postsynaptic neurons and may evoke action potential firing in them.

As the number of synapses per neuron increases during in vitro development, these processes eventually generate recurrent activity dynamics. These are reflected in periods of synchronous action potential firing across the network, so-called “network bursts” (van Pelt et al. 2005). Network bursts not only arise in vitro but can be found in organotypic slices and in the intact nervous system. Synchronous network activities such as these bursts have been implicated in learning and memory consolidation as well as synaptic transmission efficacy (Stevens and Zador 1998). It is especially involved in slow-wave sleep (Steriade and Timofeev 2003).

As neuronal networks grow, network bursts evolve depending on the spatiotemporal summation of synaptic events. To what degree of synchronization network bursts adhere to has been shown to be regulated by the degree of clustering and modularity in network connectivity (Maeda et al. 1995). These parameters, in turn, depend on the interaction of neuronal migration and neurite outgrowth during activity-dependent network development. Both of these processes contribute to increases in connectivity and thus activity in the network (Okujeni and Egert 2019). By providing an activity-offset via optogenetic stimulation, we predicted that such stimulation would inhibit development at normally premature connectivity levels and diminish the degree of neurite outgrowth as well as neuronal migration and clustering.

Figure 1 shows the evolution of firing dynamics in a neuronal network at 18 days in vitro (DIV) and at 30 DIV. Importantly, the emergence of network bursts is illustrated. At 18 DIV, sites fire in a pattern with three phases: low-level firing, synchronized firing and a silent network recovery phase. At 30 DIV, the sites fire almost exclusively synchronically in network bursts (van Pelt et al. 2005).

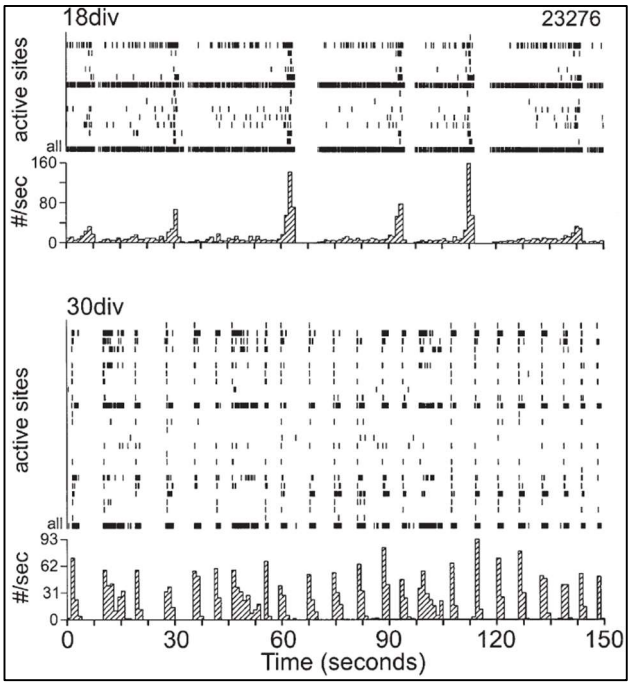

Figure 1 shows data from a cell culture at 18 DIV (top) and 30 DIV (bottom). The upper graphs show spike timings at individual recording sites as well as a trace for the summed activity, marked by "all." The lower graphs feature traces of the total number of network spikes per second. These examples illustrate the nature of network spikes with active and inactive phases. Network bursts occur during active phases. (van Pelt et al. 2005)

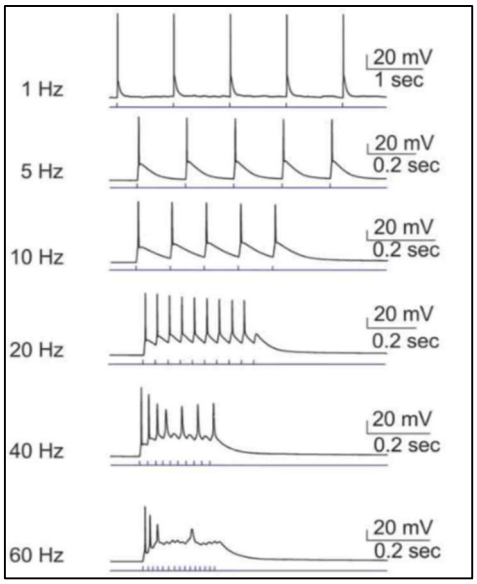

Figure 2 shows activity profiles of neurons stimulated at frequencies between 1 and 60 Hz. Spikelettes occur during constant stimulation at medium frequencies (20 Hz). In this regime, post-depolarization diminishes the availability of voltage-gated Na^+ channels by preventing them from deactivating, lowering the amplitude of APs. At high frequencies (60 Hz), this effect ultimately denies the triggering of APs and deactivates ChR2 (Lignani et al. 2013).

1.2 Optogenetics Explained

Optogenetics is a biological technique used to interact with neurons and other cell types with light. Cells are genetically altered (transfected) to express light-sensitive proteins called channelrhodopsins which function as light-gated ion channels (Nagel et al. 2002). Such ion channels regulate the membrane potentials of neurons and can bring about depolarization (Egert, Okujeni 2020). If a certain voltage potential threshold is reached, the neuron fires an action potential.

Concerning channelrhodopsins, light radiation in specific parts of the spectrum causes a conformal transformation in the protein, leading to an inflow of ions into the neuron. Such an influx depolarizes the cell. These channelrhodopsins, therefore, act as sensory photoreceptors for cells, allowing them to be activated by light. Channelrhodopsins have many variants, from being sensitive to different wavelengths of light to selectivity for different ions (Lin 2011). A variant of Channelrhodopsin 2 (ChR2) is used in this work. As ChR2 is best stimulated by light with a wavelength of 450 nm, most optogenetic researchers use blue or UV LEDs to stimulate their targets (Valley et al. 2011; Lin 2011).

In the current study, neurons are meant to be stimulated via ChR2 expressed in their membranes. This expression is regulated by the CaMKII promoter following transfection with the viral vector pAAV-CaMKIIa-hChR2(H134R)-mCherry.

Stimulation via channelrhodopsin requires precise control of the stimulation pulse duration and frequency. Due to an effect called post-depolarization, channelrhodopsins are somewhat sluggish (Lignani et al. 2013). They always stay open longer than the duration of stimulation, which allows for ion flow after stimulation. As the frequency of stimulation pulses grows, it becomes increasingly difficult for the channel to close itself. At a certain point, further increase in stimulation frequency does not increase AP firing, rather, it diminishes AP firing rates (see figure 2). Therefore, to reliably stimulate optogenetically treated neuronal networks, we must stimulate them with frequencies below 20 Hz. Likewise, stimulation with low pulse durations fails to sufficiently stimulate ChR2, as the channel is given insufficient time to open (Lin 2011).

Research into optogenetics has been on the rise in the past decade (Valley et al. 2011; McAlinden et al. 2013; Reddy et al. 2019; Keppeler et al. 2020). Usually, experimental optogenetic setups are unique and time-consuming to design and realize. A ready-made platform such as the one described in this work would save scientists much time and effort. While this first design is built for a specific experiment type, its programmable nature increases its possible

applications. Max Wechlin designed a much larger LED array for optogenetic stimulation, however, it was designed for a different use-case: stimulating single cell cultures with high stimulative resolution. This platform was never tested with real neuronal networks (Max Jürgen Wechlin 2022).

1.3 Scientific Objective

The scientific objective: a programmable platform for optogenetic long-term stimulation of neuronal networks in vitro. Studying such networks should be possible in a reliable and repeatable manner. The goal of such research is to study the changes in neuronal networks brought about by long-term stimulation. Therefore, it is vitally important that the networks be preserved after experimentation for analysis.

Why is it interesting at all to study the effects of optogenetic stimulation? The real-world use-cases of optogenetic biomedical technology are ever on the rise. Increasing the resolution in cochlear implants is one such application (Keppeler et al. 2020). Research into epilepsy is also a large sub-field of optogenetics. Concepts exist in which patients with traumatic brain injuries could be treated with optogenetics to interfere with pathological brain reorganization (Tennant et al. 2017). However, possible influences of optogenetic long-term stimulation on brain connectivity and general health are unknown. Optogenetic stimulation could also help scientists gain new insights into activity-dependent network development. So far, this has only been done by pharmacological intervention (Okujeni and Egert 2019; Okujeni et al. 2017; van Pelt et al. 2005). Optogenetics offers a cleaner, more specific stimulation paradigm.

The platform should be used for an optogenetic experiment to fully test the system. Further, the aim of such an experiment should be to study the effects of long-term optogenetic stimulation on neuronal networks. Whether the platform could carry out these experiments is discussed in the following sections, as just such an experiment was carried out to test the platform. The platform must conform to certain parameters explained in the next section.

1.3.1 Functional Requirements

The duration of the light pulse should be 10 ms, as lower durations do not reliably stimulate ChR2 (Lin 2011). The intensity of LEDs should also be such that they reliably stimulate ChR2. The conditions inside the incubator must be considered as well. Not only is neuronal activity

strongly influenced by changes in temperature, but electronics might also be damaged due to high humidity levels. A temperature of 37 °C and 95 % humidity, which can be found in an incubator, can be detrimental to sensitive electrical connections. Some sort of structure that houses and protects the electronics must be designed and constructed.

The platform must be programmable, such that stimulation patterns can be varied. Optimally, each light-emitting diode (LED) should be individually controllable and settings for the pulse duration and cycle time should be easily editable. A possible stimulation pattern (as seen in fig. 2) would be a row-by-row scheme; each well in a row of three wells would be stimulated at the same time, with the same cycle time and pulse duration. With four of these rows in a standardized 12-well cell carrier substrate, it would be possible to run experiments over 12 cell cultures with four variations simultaneously.

When considering the circuitry and control scheme for the array, many different implementations are possible. As this array uses LEDs, each diode will require an input and an output. LEDs emit light of a specific wavelength, depending on their material, when a voltage is applied in the direction of forward current flow (Oliver Paul 2020). For this to happen, the anode must have a voltage potential higher than the voltage potential at the cathode. Which exact potential difference (V_f) is required is unique to every LED and is always available on the LED's datasheet. Therefore, contacts are needed for both the anode and cathode.

A microcontroller controlling multiple LEDs will therefore require at least as many General-Purpose Input/Output (GPIO) ports as there are LEDs, plus one. Depending on the application, the cathodes of the LEDs can be linked together to use only one GPIO port acting as ground. As the size of the array grows, so does the required number of GPIO ports on the microcontroller. At some point, the microcontroller would not have enough ports to control the full array.

An alternative method is called Matrix Multiplexing. With this method, the amount of GPIO ports needed to control the array is reduced. For an array of 12 LEDs, as seen in figure 2, only 7 GPIO ports would be required. Here, the array is divided into rows and columns. The anodes of all the LEDs in a row are connected, as are all the cathodes of a column. This can be seen schematically in figure 4.

In figure 4, the switches for lines 2 and 5 are closed, meaning current can flow along the red dotted line and through LED (2,2), lighting it up. In this way, every LED in the array can be controlled.

The main draw of this method is the reduced amount of GPIO ports required. This amount can be calculated using the following formula, $n_{GPIO} = \sqrt{n_{LED}} * 2$ (1), where n_{GPIO} is the number of GPIO ports required and n_{LED} is the number of LEDs in the array.

However, one important drawback of matrix multiplexing is so-called line-flashing. This occurs when one LED in a row is turned on, the others in the same row also illuminate slightly. For example, as the microcontroller sets the anode row 2 in figure 4 to "high" voltage (5 V) to turn it on, column 5 is turned to "low" voltage (ground) to activate it. All other cathode columns (4,6) are turned to high voltage, the same level as the anode row, to disallow current flow. However, there exist small electric currents through the LEDs which should be off, resulting in faint emissions of light. This is because the potentials on the anode and cathode aren't exactly the same and allow for a small leakage current. If this light is intense enough to trigger ChR2, then the neuronal network would be stimulated outside of parameters.

Without matrix multiplexing, the required number of GPIO ports rises more quickly with the number of LEDs. This is mostly unimportant for small arrays, as the microcontrollers have enough ports for such arrays. Connecting to each LED in a 4x3 array directly would require 13 connections, 12 for the LEDs and 1 for the ground (GND) connection. Having more connections adds more complexity to the circuit.

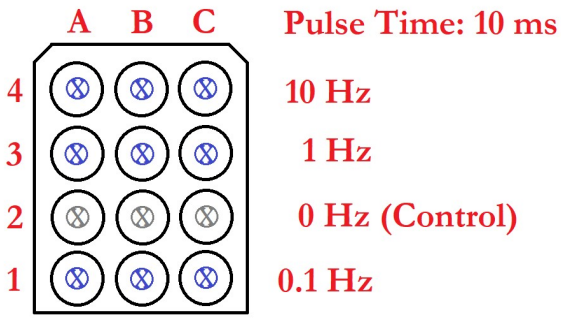

Figure 3 shows stimulation patterns used for experiments on a 12-well cell carrier

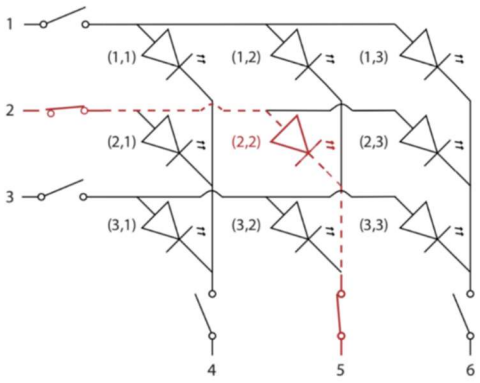

Figure 4 shows a 3x3 LED matrix connected by matrix multiplexing (Max Jürgen Wechlin 2022)

2 Materials & Methods

2.1 Technical Documentation

2.1.1 LED

One of the most important parts of an optogenetic stimulation setup is the source of light. In this work, the Nichia NSPU510CS is the LED used for the platform (Nichia Corporation 2022). It is an LED with a peak intensity at 375 nm. At this wavelength, we are operating in the UV spectrum. However, some light emitted by this diode is visible to us, shining brightly with a purplish hue. According to its datasheet, the peak radiant flux of this LED is 15.1 mW and its relative radiant intensity at 0° is 85 %. This means that an object directly above the LED will receive 15 % less energy. The true peak relative radiant intensity is actually found at 10° and drops to 0 at larger angles. If we divide the peak radiant flux by the area of a curved spherical sector (see figure 5) with its radius being the distance between the LED and the cell culture, the following equation gives us the light intensity per unit area: $I = \frac{P}{2\pi Rh}$ (2) (Paschotta 2022; Weisstein 2023). Using trigonometric identities, the value of h can be calculated, assuming the angle of the cone is 10° (see above): h ≈ 0.09 mm. Therefore, the intensity per unit area of this LED is 4.45 mW/mm^2. As the cell culture resides directly above the LED, the actual transmitted intensity per unit area is 3.78 mW/mm^2 (see above). This is sufficient to stimulate ChR2, as it only requires about 1.1 mW/mm^2 to be activated (Lin 2011).

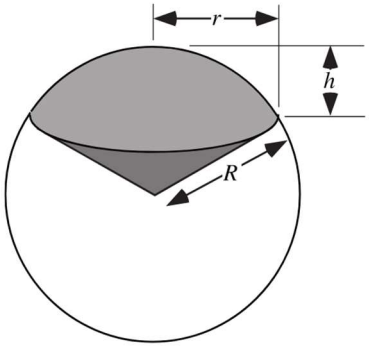

Figure 5 shows a spherical cone overlayed on a sphere. The light gray area denotes the curved spherical sector, whose area is the determinant for the transmitted intensity of light. (Weisstein 2023)

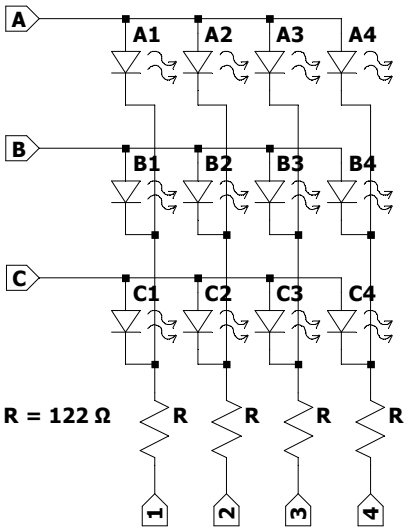

Figure 6 shows the matrix multiplexing circuit diagram of a 12 LED array. The inputs denoted A-C and 1-4 are to be connected to the digital I/O ports of the Arduino microcontroller.

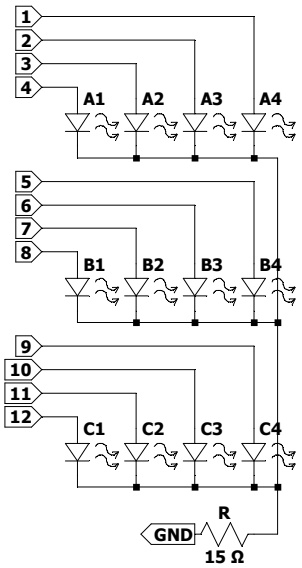

Figure 7 shows the circuit diagram of a 12 LED array with direct connections to 13 digital I/O ports of a microcontroller: 1-12 and GND.

Figure 8 shows a 12-well cell culture carrier (Falcon® 2023)

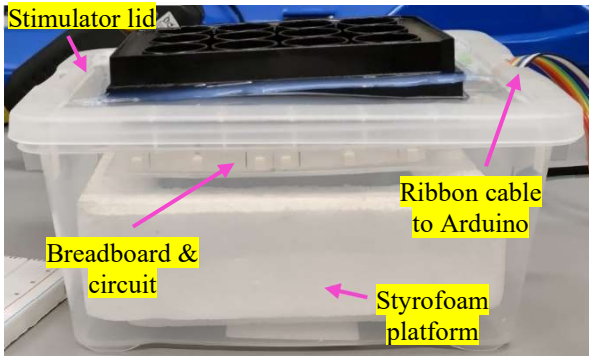

Figure 9 shows an early version of the first prototype.

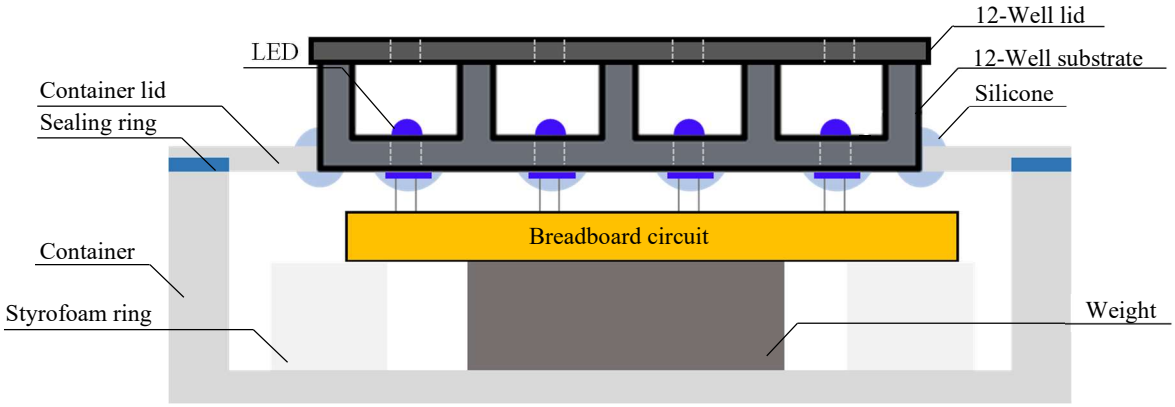

Figure 10 shows a side-on sketch of the optogenetic stimulation platform. Various functional parts are labeled.

2.1.2 Circuitry

For both stimulator prototypes, a simple breadboard substrate was used, whereupon jumper wire circuitry was built. The circuit diagram for the first prototype can be seen in figure 6. Thusly, the LED array is connected via matrix multiplexing. Importantly, the spacing of the LEDs and their respective connections on the circuit were determined by the separation of the wells on the 12-well plate, for which this platform was designed and out of which a part of the electronics housing is made. Which connections lead to which GPIO port on the microcontroller is unimportant, as the pin functions are set in the code.

2.1.3 Microcontroller

In order to run the circuit and every LED at varying frequencies, a microcontroller was required. An Arduino Uno was chosen for this role, as it had enough GPIO ports for both circuits and it made interfacing with the circuit simple. Using C++, programs could be written to the microcontroller for it to output to its digital GPIO ports. Connections from these ports to the circuit were made via a 2-meter-long ribbon cable. Figure 2 shows the required stimulation patterns which were implemented into C++ code. Programs were written for both matrix multiplexing and direct LED connection circuits.

2.1.4 Construction

The platform hinged on compatibility with Falcon brand 12-well cell carrier substrates (figure 8). As these substrates were designed to be stackable, it made sense to incorporate one of these substrates as the interface between the platform and a cell carrier. Using one of these as a base, the rest of the optogenetic stimulation platform was conceived. Each well required an LED for stimulation, so holes were drilled into the centers of each. An identical hole was drilled into the cell carrier lid to more accurately aim and further restrict the light transmitted.

The cell carrier needed to be painted black, as each neuronal network was to be stimulated individually, without influence from other LEDs or other light sources. The interior of the incubator is normally dark when closed, so the only source of illumination would be the platform itself. Thus, it made sense to paint the normally clear cell carrier black. This was done with a coat of black spray paint.

The housing of the electronics was one of the most important components. Firstly, the electronics must be contained to make the platform more robust and secondly, to shield sensitive parts from deteriorating due to humidity. A role which was to be filled by a plastic container, inside which resided the breadboard, circuitry and a stainless-steel weight. The cell carrier, prepared as described above, needed to be integrated into the container lid somehow.

A hole was cut into the lid of the container, with a circular saw, fitting the altered 12-well cell carrier. Silicone sealed the gap between the container lid and the cell carrier. The LEDs were inserted into the holes on the cell carrier and oriented such that they would have the correct polarity when connected to the circuit. Then silicone was used to bind the LEDs to the underside of the cell carrier. This allowed the LEDs to be connected to the circuit without compromising the protection of the housing or the transmission of light.

The finished stimulator lid consisting of the 12-well cell carrier, container lid and LEDs was now monolithically connected to the circuit. This then was placed inside the container, atop a platform inside the container such that the circuit did not hang freely from the lid and was supported when the lid was installed on the container.

In the first attempt, a container made of polypropylene, a thermoplastic polymer, was used. Connecting the lid with the cell carrier failed, as the material was too flimsy and easily broke the silicone bond. This first version can be seen in Figure 9.

As the search for a new container began, the need for a sealing ring around the edge of the lid was recognized. This would make the seal more airtight. A second container was acquired, an IKEA 365+ model with a silicone sealing ring built in. This type of container was made of PP-R, which is a copolymer of polypropylene and at least one comonomer. After a hole was cut into the lid, the carrier was attached with silicone paste from both sides and to the LEDs from the inward side. After drying, the container proved to be both robust and sealable. A piece of Styrofoam was cut to fit in the container and act as a stable platform for the circuitry to rest on. A small metallic cylinder was used as a weight to make the platform more stable. Figure 10 shows a side-on schematic view of the prototype design.

2.1.5 Second Prototype

The second prototype benefited from lessons learned during the construction of the first. Before drilling the holes into the cell carrier, the substrate and the lid were taped together so that the holes would be lined up better than on the first prototype. Before painting, the carrier was

soaked in isopropyl to thoroughly clean the surface. A primer layer was applied before the black paint for better adhesion, durability, and color intensity. Figure 11 showcases the second prototype's construction.

While the first prototype's circuitry was connected via matrix multiplexing, the second prototype had its LEDs directly connected to the GPIO ports of the microcontroller via a ribbon cable. This was done to test if this alternative circuitry was viable and in case the matrix multiplexing method failed. The circuit diagram used can be found in Figure 7. Both circuits were built on a breadboard and can be seen in Figure 12. The finished prototypes are depicted in Figure 13.

2.1.6 Programming

Programming of the microcontroller was done in C in the Arduino IDE. First versions of the program were simply repeating loops of code. These loops caused every LED in the array to flash, one after the other. In this way, every culture on the array would be stimulated uniformly. This code can be found in the auxiliary material as "Full Array Pulse". However, this approach could not scale to output the required stimulation pattern for the experiment, as. Therefore, a different method was required. With help from an online tutorial, a new method was conceived. Using the three timers built-in to the microcontroller, the exact points in time when an LED should pulse can be determined. These so-called "timer interrupts" trigger when a counter matches a specific stored value, then resets this value and continues the count. By setting this match value and the speed of timer increments, it is possible to set the frequency of timer interrupts (Ghassaei 2012). This is easily translated to the frequencies required in the stimulation pattern. As the two stimulators had two different circuitries, two distinct programs had to be written. These can be found in the auxiliary materials.

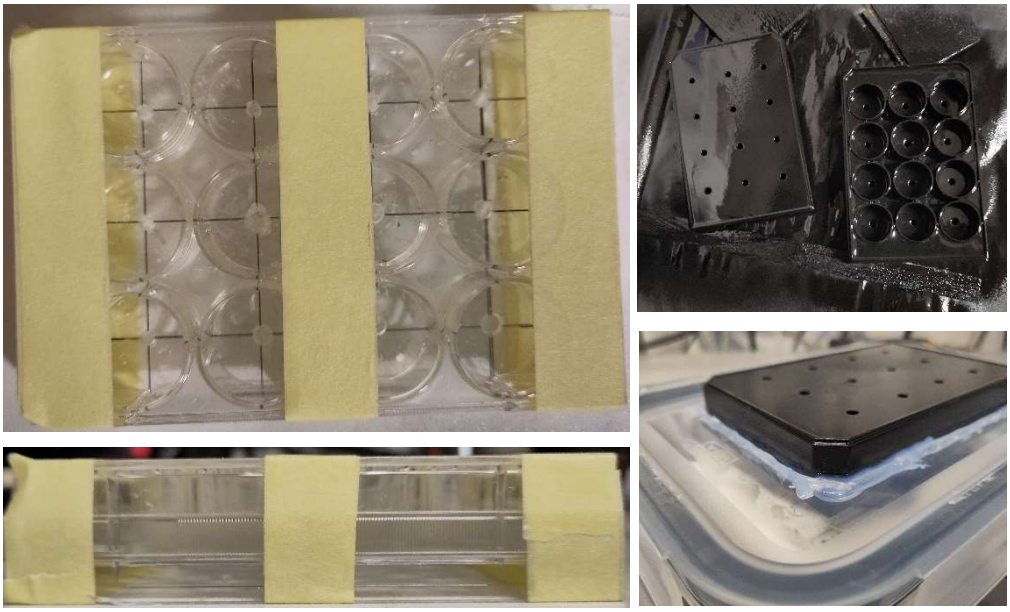

Figure 11 includes four images taken during construction of the second prototype. Left: Cell carrier substrate and lid are taped together for better alignment during drilling of through-holes. Top right: Cell carrier is spray painted. Bottom right: Silicone is applied to bind the carrier to the container lid.

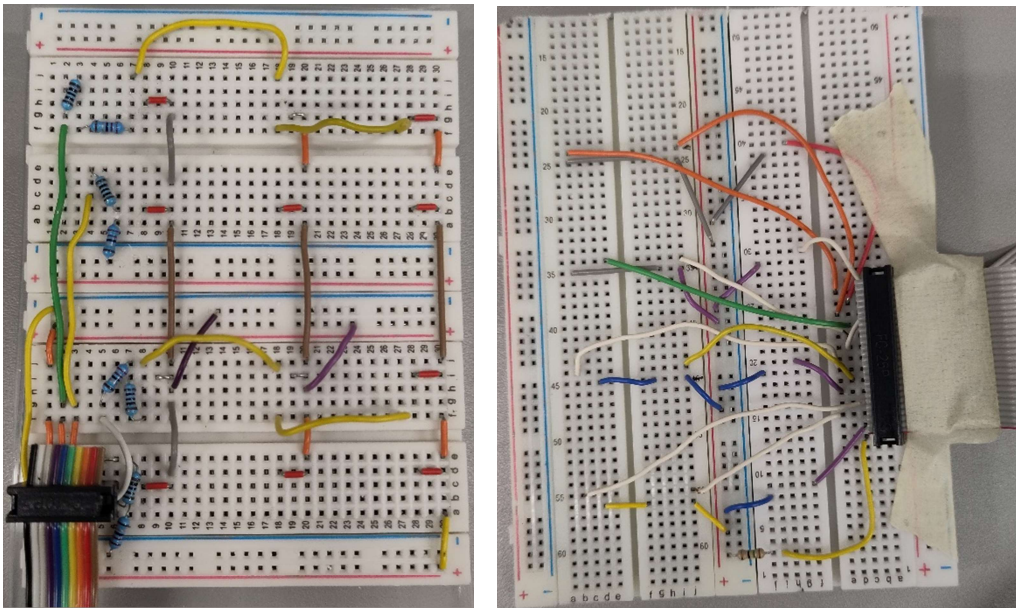

Figure 12 includes two images of the circuits controlling the LED arrays. Left: Circuit for the first prototype utilizing matrix multiplexing. Right: circuit for the second prototype.

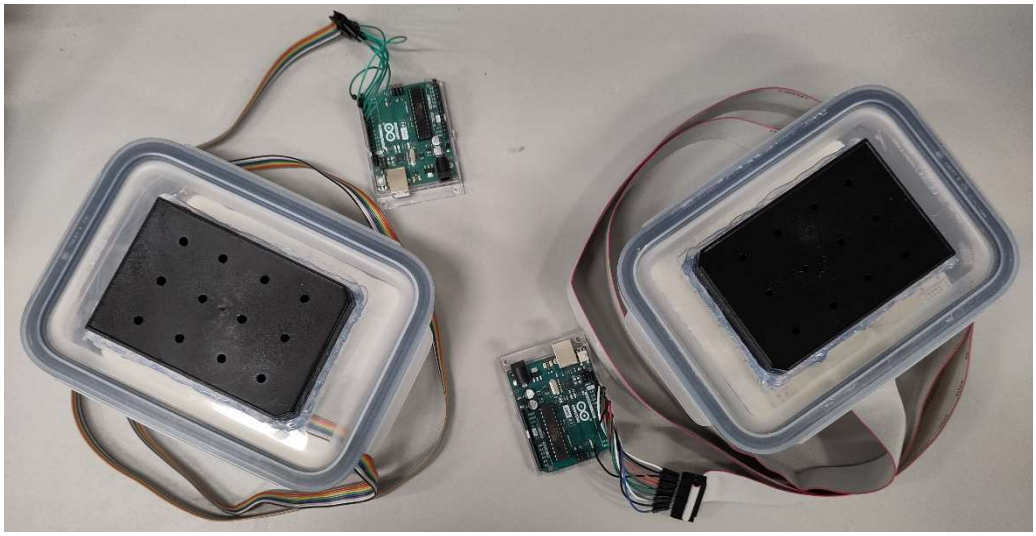

Figure 13 shows both finished prototype stimulation platforms and their Arduino Uno microcontrollers. Left: first prototype with matrix multiplexing circuitry. Right: second prototype with direct connection circuitry.

2.2 LTS Experiment Documentation

2.2.1 Overview

From the outset, three long-term stimulation experiments were planned. The first was cancelled due to time constraints; the first prototype was not ready on time due to the above-mentioned issues with the container's material properties. The second experiment did not provide any useful data. A mistake during transfection meant only three neuronal networks were transfected, causing all but three networks to not express ChR2. The three that were transfected were part of the control group, however, and therefore were not stimulated. The third and final experiment proceeded without incident.

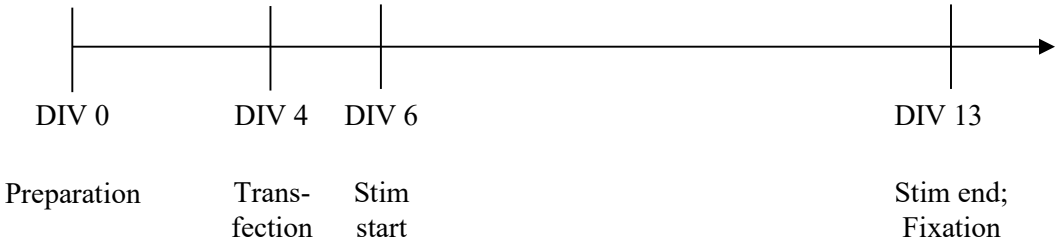

Figure 14 shows a timeline of the final LTS experiment

2.2.2 Timeline

A timeline of steps in the experiment can be found in figure 14. Cell cultures PID509 CID7670 (abbreviated as Cell Culture 1, CC1) & CID7668 (CC2) were prepared on 02.12.2022 following procedures described in Dr. Okujeni's works (Okujeni et al. 2017; Okujeni and Egert 2019). In short, there were three variations of cultures on each 12-well cell carrier: four cultures treated with 1 mM PMA, four cultures treated with 1 mM Gödecke6976 (GOE) and four otherwise untreated cultures were used as controls. GOE and PMA are PKC antagonist/agonist. Protein Kinase C (PKC) is an enzyme that regulates neurite growth and cell migration among other parameters. PKC agonist PMA promotes clustering of neurons, thereby reducing neurite density, while PKC antagonist GOE does the opposite (Okujeni 2012).

CC1 and CC2 were transfected on DIV 4 with pAAV-CaMKIIa-hChR2(H134R)-mCherry, dubbed "mCherry," to express ChR2.

Two days later, 6 DIV, the stimulators were placed into the incubation chamber and oriented such that their ribbon cables could easily exit the chamber. CC1 was placed on S1 while CC2 was placed on S2. The platforms were plugged in and the time and date for the beginning of the experiment was noted: 08.12.2022, 10:24 for CC1 and 10:39 for CC2. Stimulation was interrupted on DIV 10 for medium exchange. The stimulation and experiment ended at 13 DIV, 15.12.2022, at 11:24 for CC1 and 11:34 for CC2. The networks had been transfected for nine days and exposed to LED radiation for a week.

2.2.3 Immunohistology & Microscopy

Directly after completing the stimulation experiment, an immunohistology was performed to preserve the networks for photography and analysis. The antibodies used for this procedure were Rabbit-anti-NeuN, for marking neurons, Mouse-anti-Neurofilament, for marking neurofilaments, Goat-anti-Mouse-Cy2 and Goat-anti-Rabbit-Cy3, for phosphorescence, and DAPI, for marking nuclei. These were each added in dilutions of 1:200 with glucose solution and produced by Abcam. The plasmid mCherry was added during culture preparation in dilution of 1:1000 with glucose solution and marks areas of expressed channelrhodopsin.

Photographic microscopy of the preserved networks was performed with a Zeiss Axio Observer Z1 and Zeiss Zen 2013 software. Illumination of the networks was provided by a Colibri LED controller with 365 nm (nuclei), 470 nm (neurons), 555 nm (neurofilaments) and 625 nm

(mCherry) wavelength LEDs. Areas of 4 mm^2 were photographed. Morphometric analyses were then performed on the captured micrographs in MATLAB.

2.2.4 Analysis

Morphometric analyses were performed on micrographs of the networks using MATLAB code kindly provided by Dr. Samora Okujeni. Among analyzed parameters were the clustering of neurons via the Clustering Index (CI), neuron and glia density, neuron ratio as well as axon length. Neuron and glia densities are important, as there are direct connections between cell death, clustering, and cell densities. We determined the glial density indirectly from the fraction of nuclei stained with DAPI that did not show a neuron-specific nuclear stain. Measuring glial cell density is also important because these cells were not transfected. If there is a difference in densities between the two, that is direct evidence of LED stimulation affecting transfected neurons.

The Clustering Index of a neuronal network is a measure of how highly clustered its neurons are. As stated above, networks treated with PMA have stronger neuron clustering while GOE-treated networks have a largely homogenous spread of neurons. The CI of a neuronal network is calculated as described in (Okujeni et al. 2017): the nearest neighbor distances (NND) between neurons are measured and averaged ($\overline{NND}_{Real}$). Then a random point pattern with the same density is created. Simulated neurons are inserted at random points, but only if a minimum distance to other neurons is observed. This distance is usually around 10 µm. These points are added to a list until the desired point density is reached. From this list, the nearest neighbor distances of the simulated neuronal network are calculated. Next, the average of these is calculated ($\overline{NND}_{Sim}$). This is repeated as many times until the standard error is less than 0.01. Finally, the CI is calculated: $CI = \frac{\overline{NND}_{Real}}{\overline{NND}_{Sim}}$ (2)

In short, the CI is the ratio between the average observed and expected NND. A CI of 0 would infer a fully clustered network, meaning the NND is equal to the minimum distance between neurons. A CI of 1 infers a completely random neuron distribution (Okujeni et al. 2017).

2.3 MEA Experiment Documentation

The purpose of this experiment was to analyze the response of an optogenetically treated neuronal network to UV light stimulation. The basic setup of the experiment was this: a small table made of plastic and screws (figure 15 B)) which held an LED. This was hooked up to a circuit that mimicked an LED array similar to the first stimulator prototype (figure 15 A)). This table sat directly beneath the MEA tray such that the culture was stimulated from below (figure 15 C)). The MEA responses were recorded using MC Rack.

Cell culture PID508 CID7656 (CC3) was prepared on a standard micro-electrode array (MEA) with PMA as described in Dr. Okujeni's works (Okujeni 2012; Okujeni et al. 2017). Transfection occurred on DIV 7. Cell cultures PID509 CID7654 (CC4) and PID509 CID7665 (CC5) were prepared in the same manner and transfected on DIV 4.

At 22 DIV, CC3 was stimulated via LEDs (10 ms pulse at 0.2 Hz) from a distance of 6.5 mm. The MEA response from the culture was measured. This culture was fixed on DIV 27 and an immunohistology was performed.

For the second experiment, MEA responses of CC4 and CC5 during LED stimulation (10 ms pulse at 0.2 Hz) were measured at three different heights (6, 18 and 21 mm) on DIV 12. The cultures were fixed on DIV 17 and immunohistologies were performed for both.

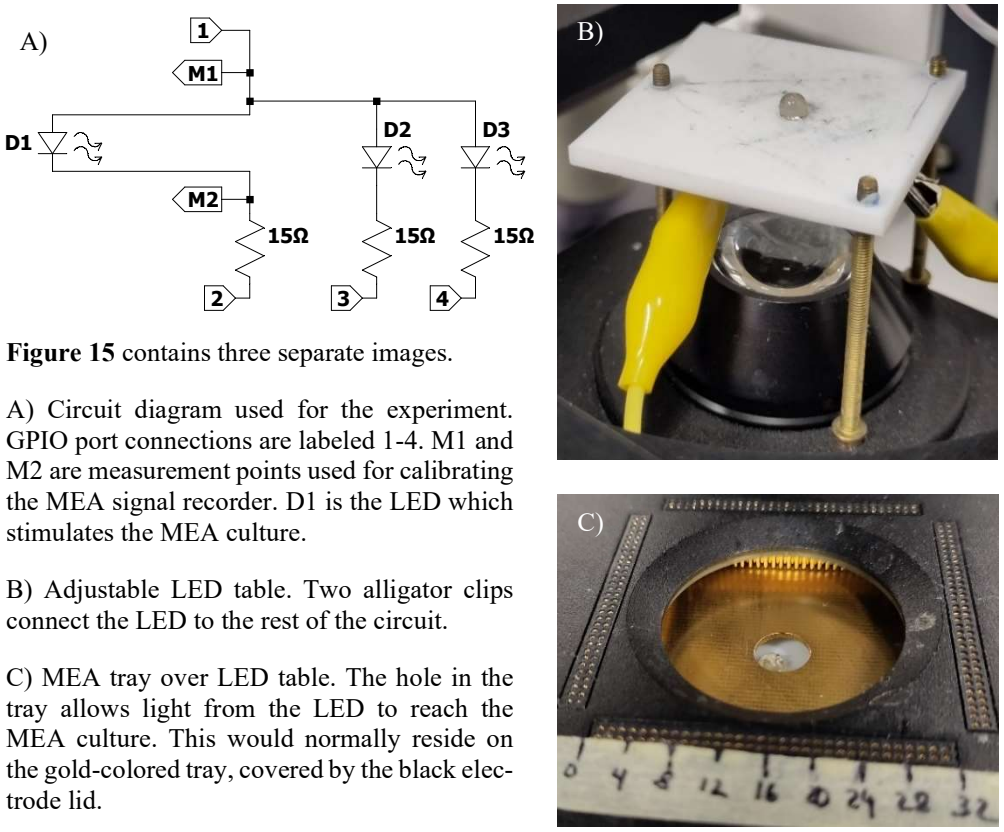

Figure 15 contains three separate images.

A) Circuit diagram used for the experiment. GPIO port connections are labeled 1-4. M1 and M2 are measurement points used for calibrating the MEA signal recorder. D1 is the LED which stimulates the MEA culture.

B) Adjustable LED table. Two alligator clips connect the LED to the rest of the circuit.

C) MEA tray over LED table. The hole in the tray allows light from the LED to reach the MEA culture. This would normally reside on the gold-colored tray, covered by the black electrode lid.

3 Results

3.1 LED Stimulation Platform for Optogenetic LTS

First of all, the programs written for the stimulators needed to be tested to ensure the cell cultures would be stimulated correctly. They were tested and shown to function on the stimulators as designed. S1 was tested in the incubator during normal function overnight with the array flashing. It was confirmed to be undamaged; the array had continued flashing.

Temperature and humidity were measured from the inside of the prototype with a sensor. At the beginning of the experiment, the temperature inside the stimulator was 21 °C with a humidity of 40 %. When the stimulator was removed approximately 24 h later, the sensor showed a temperature of 37 °C and a humidity of 42 %.

During the first, unsuccessful experiment, it was found that the connections between the ribbon cable and the microcontroller were unstable, leading to a weakening in LED intensity over time. These were exchanged for jumper cables before the second experiment, which greatly increased the reliability of the LED's intensity.

Concerning the effectiveness of the LEDs at stimulating neuronal cultures, MEA recordings of CC3 showed activity spikes directly following LED illumination.

3.2 MEA Experiment Results

In order to determine whether LED stimulation evoked neuronal activity in optogenetically treated neuronal networks, we stimulated neuronal cultures grown on MEAs. The LED was placed the same distance from the culture as in the stimulators (6 mm) and recorded spiking activity.

MEA data collected from experimentation on CC3 showed that the LED successfully stimulated neurons in the network. The recorder for the 256-electrode MEA was able to readout neuronal signals in real time during LED stimulation sessions. An overview of the recorded electrode signals can be seen in figure 16. Figure 17 shows data from single electrodes. These

are meant to be representative of typical signal types recorded by the MEA. Some electrodes supplied noisy data or did not show spiking activity (figure 17 D)). The photoelectric effect caused many electrodes to record false spiking activity. An example of this can be found in figure 17 B). A typical network burst with a short component immediately following the stimulus, a silent period, followed by a long late component can be seen in figure 17 A). Figure 17 C) depicts a network burst without an early component.

Figure 18 is the waveform of recorded signal data from neuron firing activity around a single electrode. This depicts a classical action potential. Figure 19 is likewise a waveform of recorded electrode data; however, this signal is indicative of the photoelectric effect.

Experimentation with CC4 and CC5 yielded no clear evidence of stimulation.

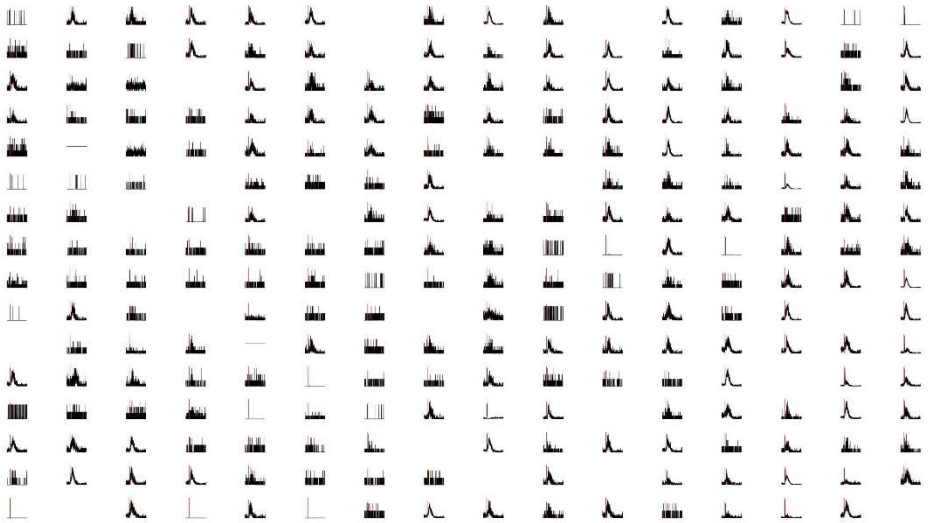

Figure 16 shows PSTHs of neuron firing activity recorded around the electrodes of a MEA. Each graph corresponds to activity around a single electrode. The graphs are arranged according to the electrode's position in the array. The red lines denote the instant of stimulation.

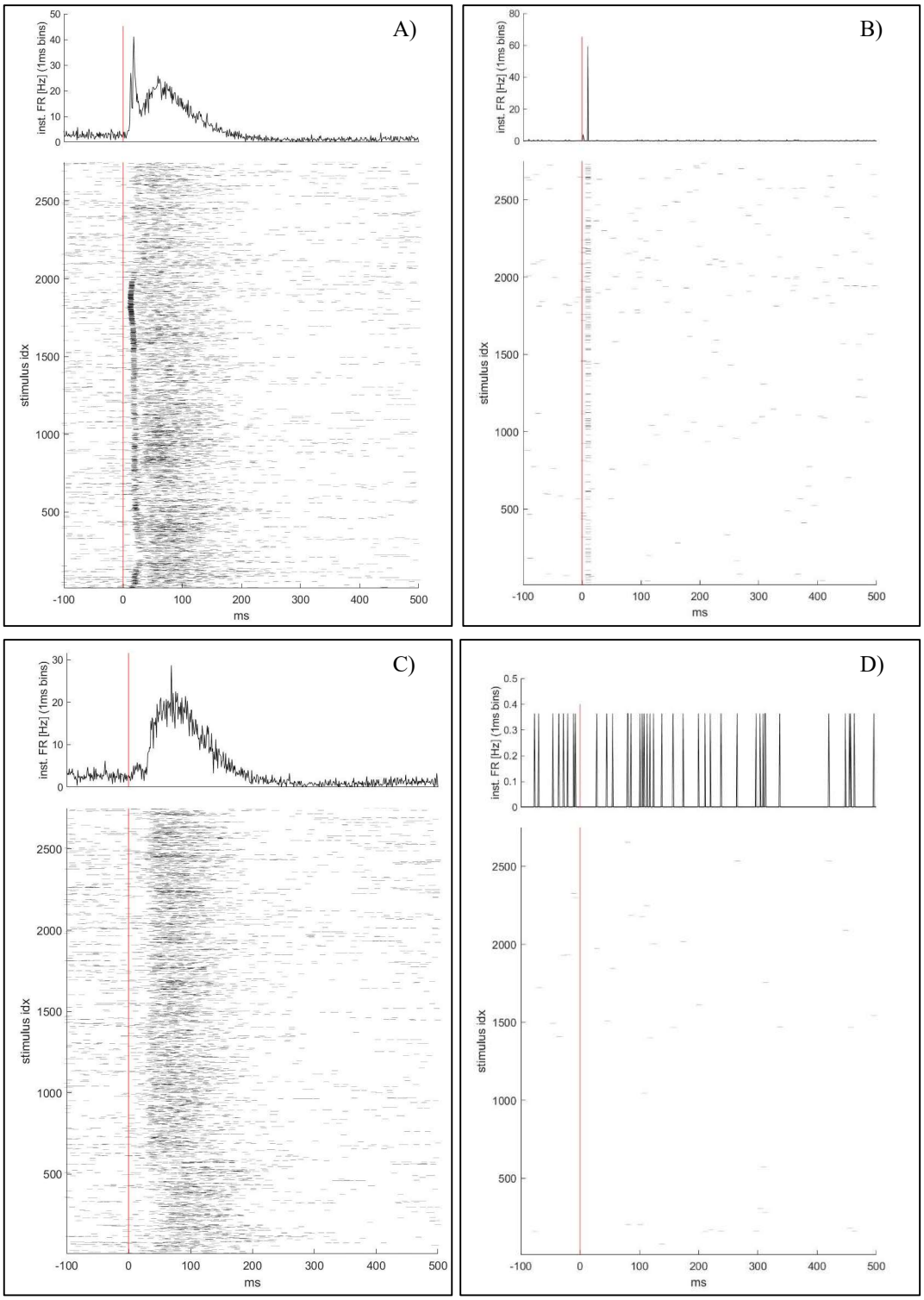

Figure 17 shows four distinct graph pairs. In each pair, the bottom graph shows individual signals recorded by the electrode while the top graph is a peristimulus time histogram (PSTH) of data from the bottom graph. A) is indicative of a network burst with an early and late component; B) is indicative of the photoelectric effect inducing a signal on the electrode; C) is indicative of a network burst without an early component; D) is indicative of the absence of spontaneous, directly or indirectly elicited spiking activity. The red line in each graph depicts the precise point in time of the LED pulse.

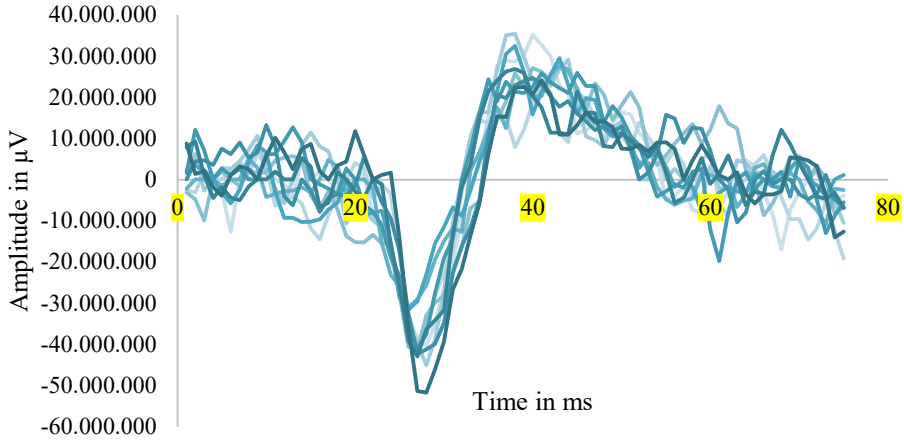

Figure 18 depicts the signal recorded by a single electrode in the MEA. This corresponds to the firing activity of neurons in the area around the electrode. The different lines denote unique responses; in total there are 10 recorded signals overlayed in t

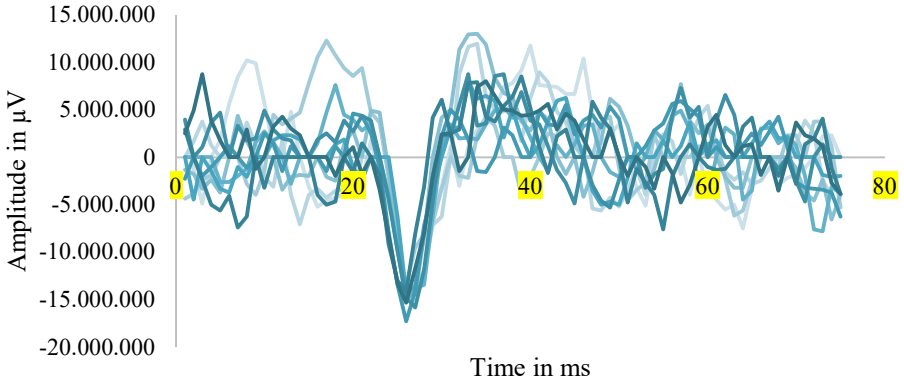

Figure 19 depicts the signal recorded by a single electrode in the MEA. This corresponds to the the waveform induced by the photoelectric effect. The different lines denote unique responses; in total there are 10 recorded signals overlayed in this graph.

3.3 LTS Experiment Results

In order to analyze the neuronal networks, micrographs had to be made of the cultures. Immunohistology allowed for these micrographs; areas of 4 mm^2 of each neuronal network were photographed after experiment completion. These originally grayscale images were edited and given false colors to better differentiate between cellular structures. Figure 20 is a grid of such images showing 1mm^2 sections of each network arranged to the network's position in the array. Figure 21 shows a close-up of a control group network and exemplifies the fact that the algorithm written to identify neurons is imperfect; some neurons in this image are not marked. This is because there is a continuous intensity spectrum of neuronal nuclei, which makes it

impossible to define a non-ambiguous threshold to separate immunoreactive cells from the background.

Morphometric analyses to study developmental changes in the neuronal cultures were performed on CC1 and CC2's micrographs using code scripts for MATLAB provided by Dr. Samora Okujeni. Neuron density, glial density, neuron fraction, the clustering index (CI) and axon length per neuron were identified by the program. See figures 22 and 24 for absolute results and figures 23 and 25 for normalized results. All results are depicted as boxplots.

When taken together, much of the data from analyses of both cultures are inconclusive or show no significant impacts of stimulation. It appeared as if the CC2 networks had different reactions to stimulation than the CC1 networks.

3.3.1 Densities

Concerning the neuron densities of the networks, it appears as if CC1's PMA cultures are generally denser than those of CC2 (figures 22 A) and 24 A)). In fact, both cell culture groups have much higher neuron densities for cultures treated with GOE than expected.

Glial densities (figure 22 B)) for CC1 are spread out between 400 – 1200 mm^{-2} while those of CC2 (figure 24 B)) are between 500 – 800 mm^{-2}, with the notable exception of the GOE cultures, which range from 800 – 1400 mm^{-2}. Interestingly, this does not appear to have an effect on the neuron fraction (figures 22 D) and 24 D)), as these are roughly the same across cell cultures.

3.3.2 Clustering Index

The measured CI of CC1 PMA cultures showed they tended to have heightened neuronal clustering; their CIs were between 0.6 – 0.9. The other cultures (controls and GOE) had higher CIs and were on par with one another at around 0.7 – 1 (figure 22 C)). CC2's cultures were all in the same region of the CI; also between 0.7 and 1, with the notable exception of the PMA culture at 0.1 Hz with a CI around 0.6. Such clustering indices are uncharacteristic for these types of cultures (Okujeni et al. 2017).

Although PMA cultures tend to have heightened neuronal clustering due to PMA being a PKC agonist, and therefore a CI of around 0.5 – 0.6; when we would expect GOE cultures to score significantly higher than controls.

3.3.3 Axon length

The relationship between axon length and stimulation frequency varies between the two cell culture groups. While CC1's axon lengths seem to decrease for low frequencies and increase for high frequencies (figure 21 E)), CC2 tends towards a constant decrease in axon length with increasing frequency (figure 23 E)).

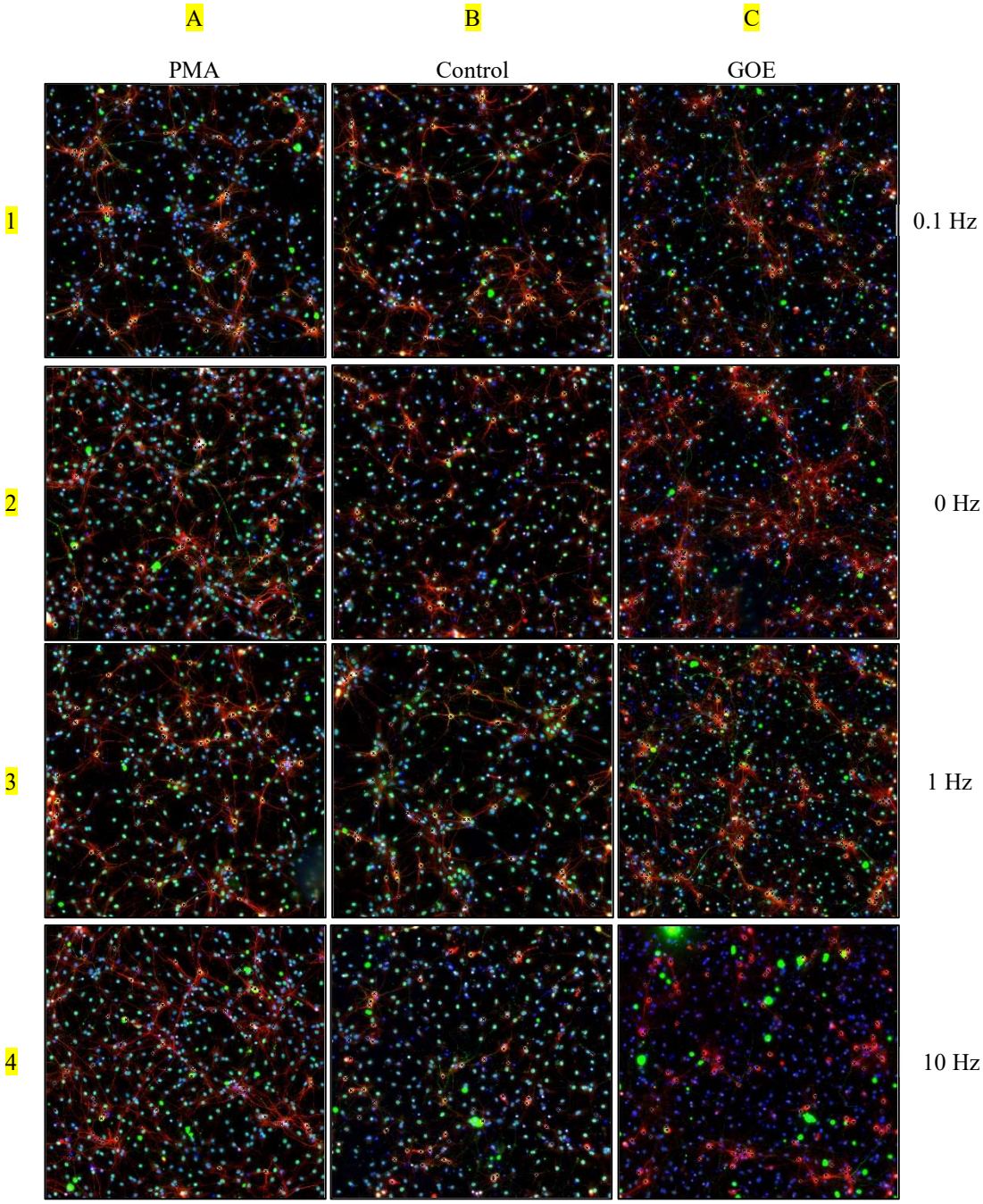

Figure 20 is a grid of false-color images taken from each neuronal cell culture in C2. They are arranged according to their position on the 12-well cell carrier during the experiment. Each image represents a region of the corresponding neuronal network about 1 mm^2 in size. Image artefacts are common and can be identified as large, blurry spots; for example, the large green spot at the top left of image C4.

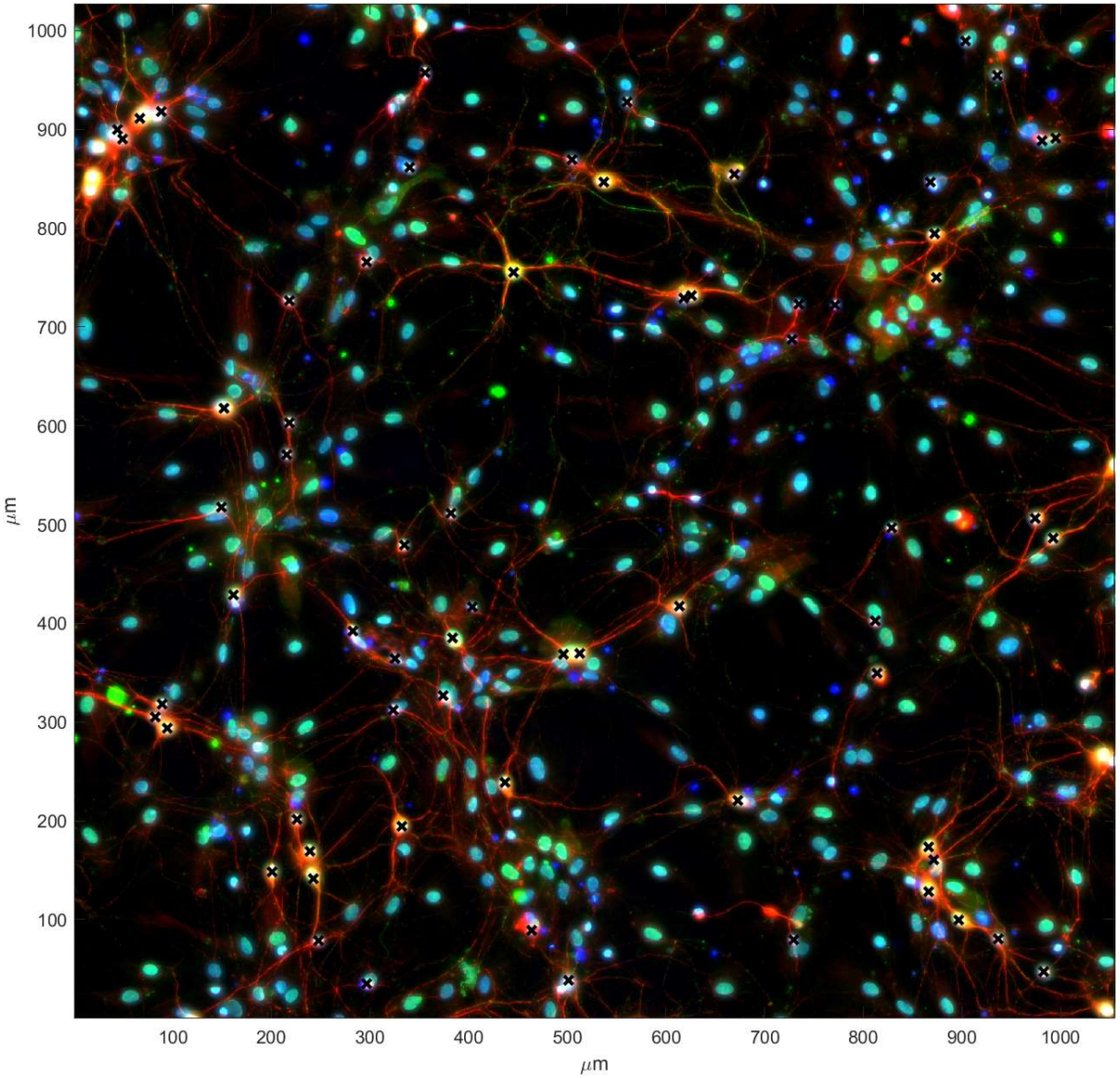

Figure 21 shows a close-up false-color image of a 1 mm^2 region of neuronal network B3 (preparation CC2). This culture was stimulated at 1 Hz.

Red lines mark dendrites (Rabbit-anti-NeuN), green lines mark axons (Mouse-anti-Neurofilament), blue/green spots mark nuclei (DAPI). The black crosses mark neurons detected by the analysis algorithm. Note, some neurons are not detected, for example in the top left.

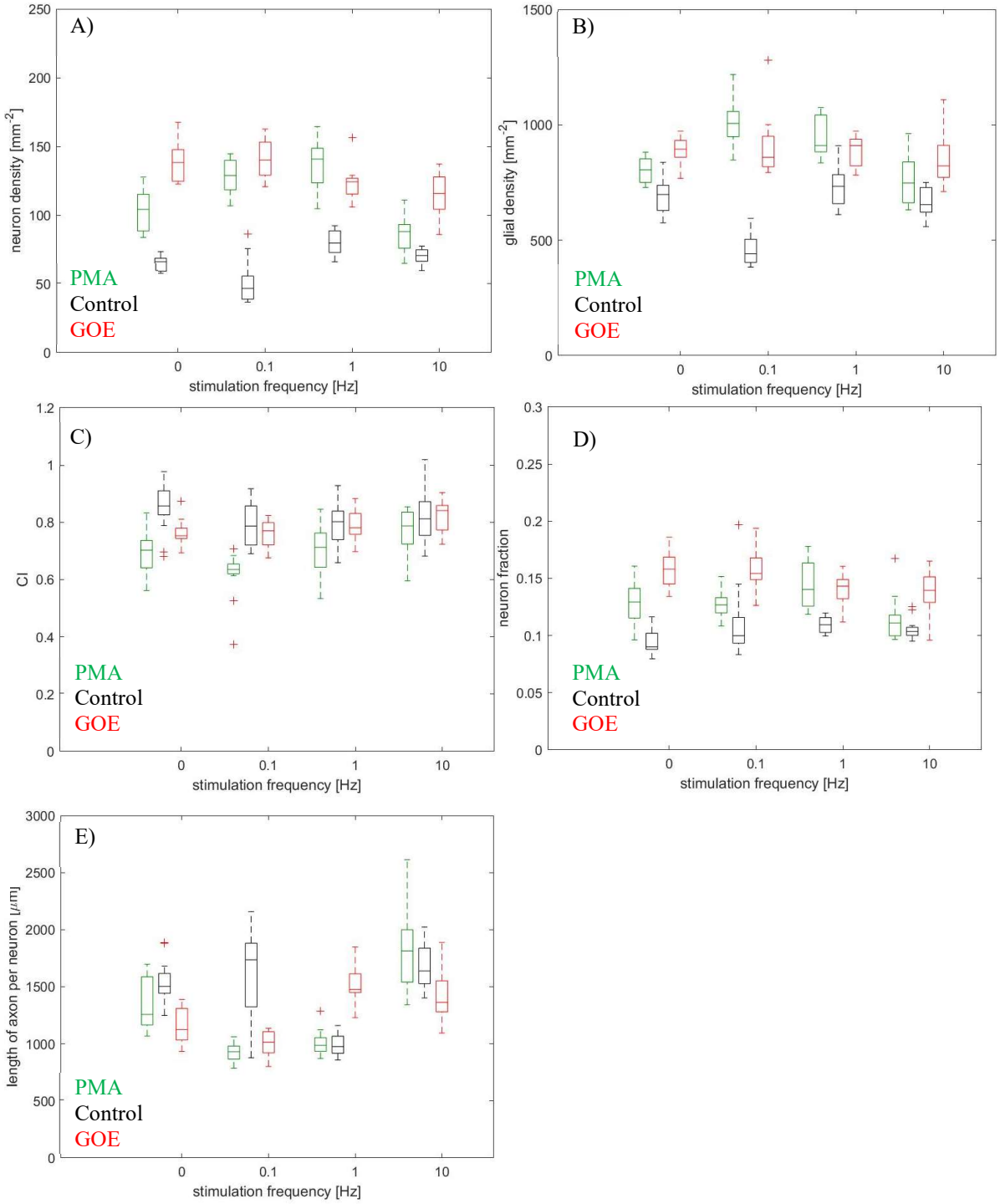

Figure 22 hosts multiple boxplot diagrams for results from morphological analysis of CC1. All parameters are displayed against the stimulation frequency, A) displays neuron density; B) displays the glial density; C) displays the CI; D) displays the fraction of neurons out of all cells in the network; E) displays the length of axons. The boxplot representations of data from each culture are displayed and colored according to treatment with PMA, GOE or neither.

These are the results of an unpaired single-sample student's t-test. Data collected from CC1. Asterisks denote statistical significance, one for $p < 0.05$, two for $p < 0.01$ and three for $p < 0.001$. Outliers are marked by crosses.

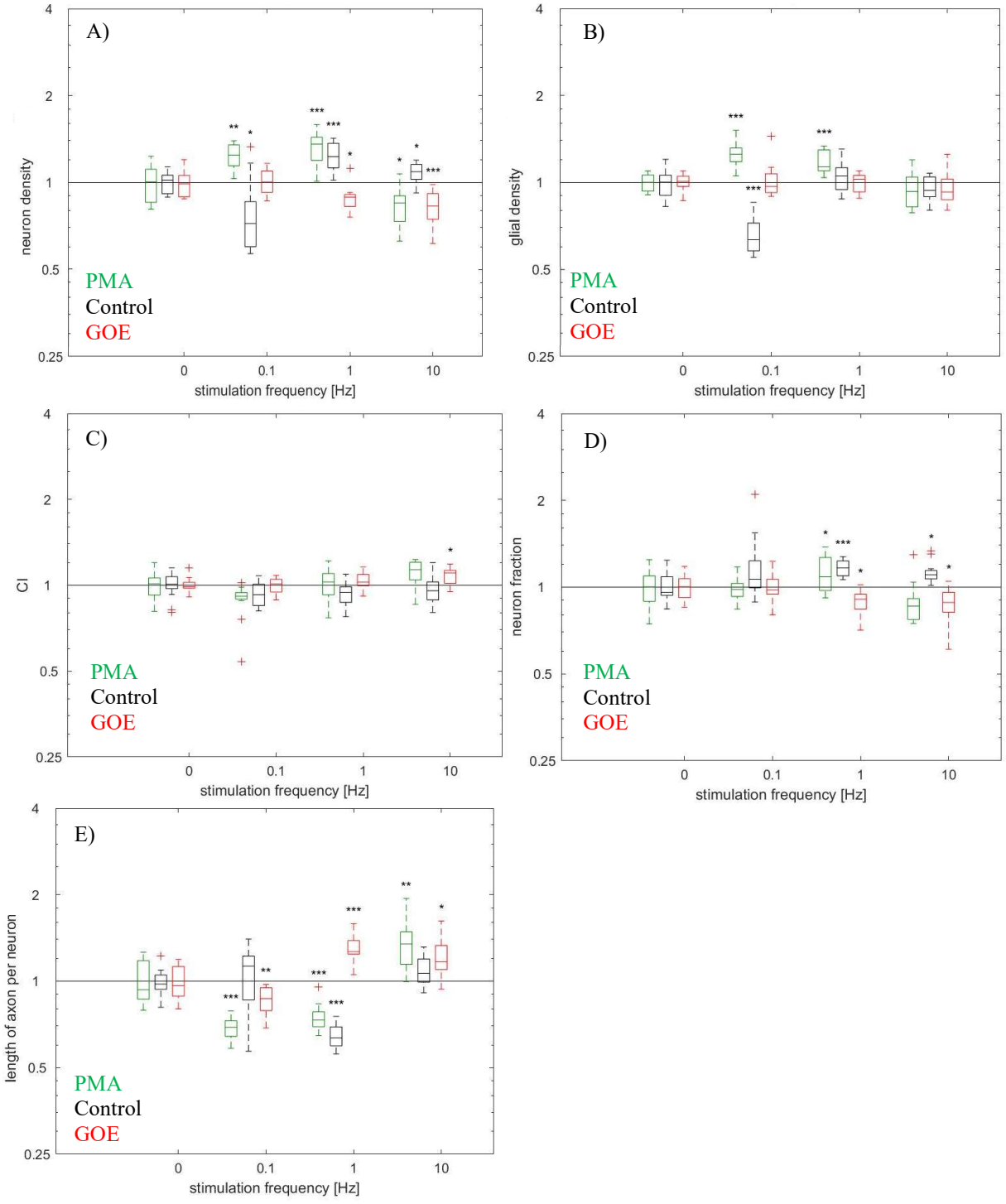

Figure 23 hosts multiple boxplot diagrams for results from morphological analysis of CC1. All parameters are normalized around the first control culture and displayed against the stimulation frequency, A) displays neuron density; B) displays the glial density; C) displays the CI; D) displays the fraction of neurons out of all cells in the network; E) displays the length of axons. The boxplot representations of data from each culture are displayed and colored according to treatment with PMA, GOE or neither.

These are the results of an unpaired single-sample student's t-test. Data collected from CC1. Asterisks denote statistical significance, one for $p < 0.05$, two for $p < 0.01$ and three for $p < 0.001$. Outliers are marked by crosses.

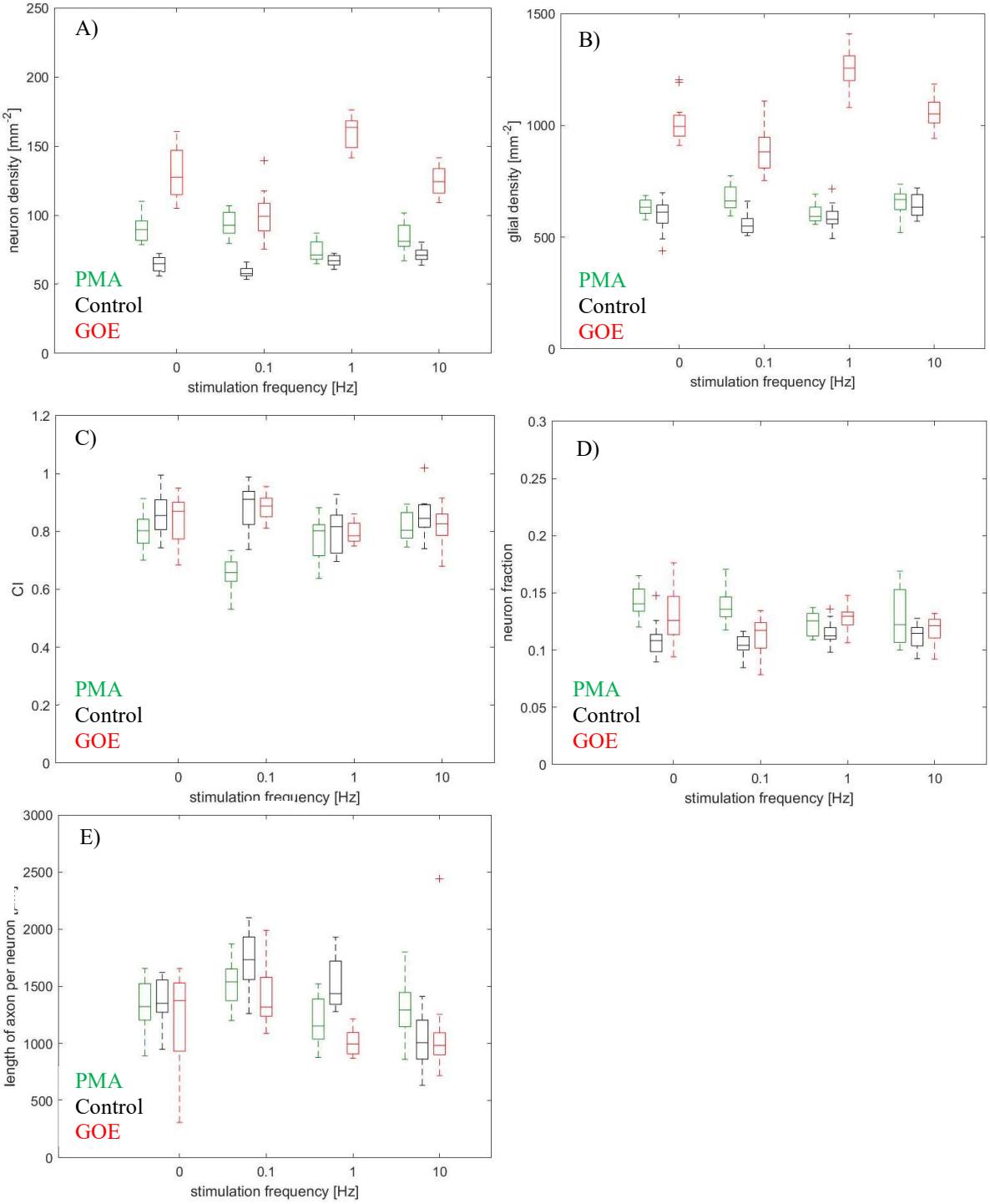

Figure 24 hosts multiple boxplot diagrams for results from morphological analysis of CC2. All parameters are displayed against the stimulation frequency, A) displays neuron density; B) displays the glial density; C) displays the CI; D) displays the fraction of neurons out of all cells in the network; E) displays the length of axons. The boxplot representations of data from each culture are displayed and colored according to treatment with PMA, GOE or neither.

These are the results of an unpaired single-sample student's t-test. Data collected from CC2. Asterisks denote statistical significance, one for $p < 0.05$, two for $p < 0.01$ and three for $p < 0.001$. Outliers are marked by crosses.

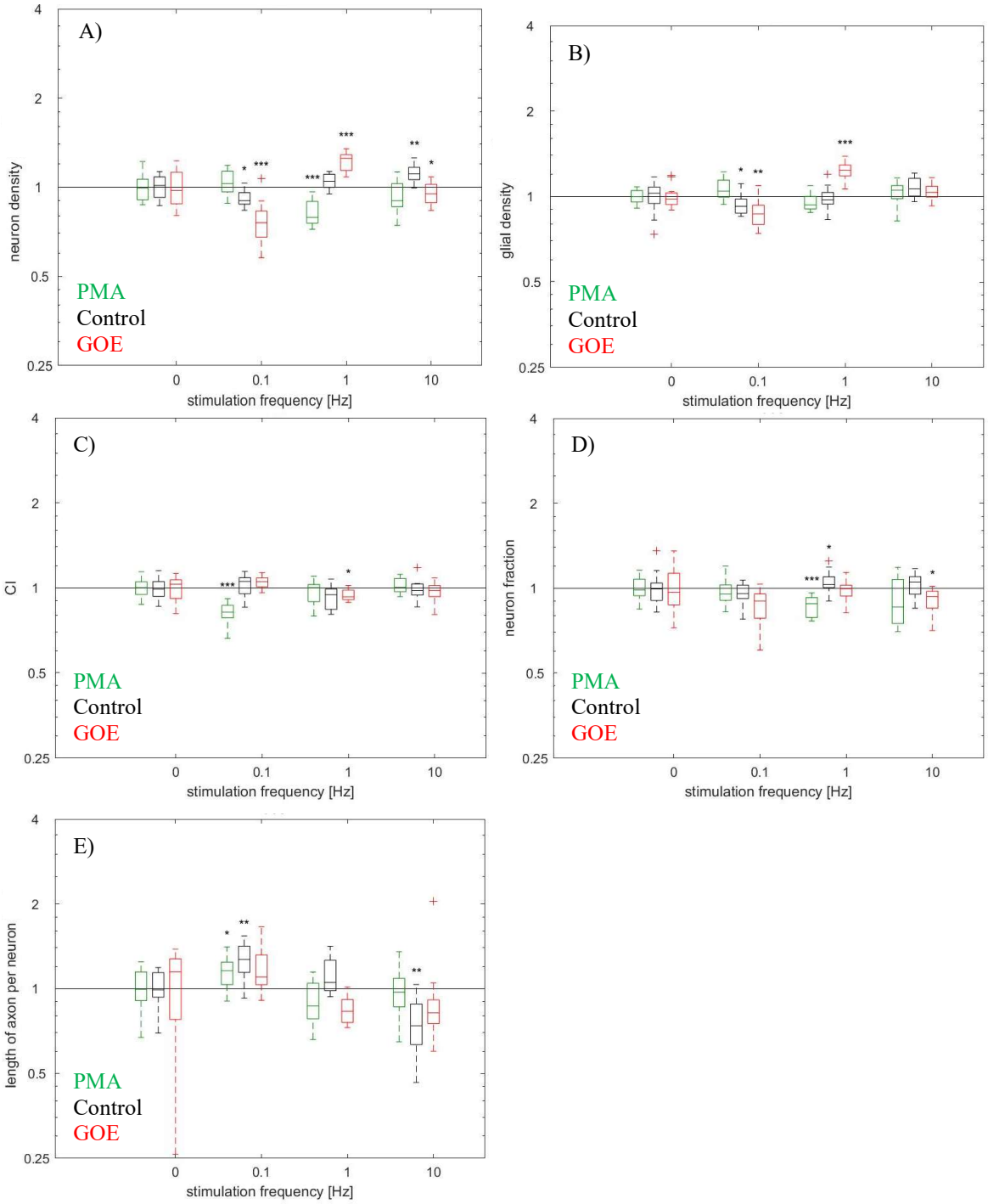

Figure 25 hosts multiple boxplot diagrams for results from morphological analysis of CC2. All parameters are normalized around the first control culture and displayed against the stimulation frequency, A) displays neuron density; B) displays the glial density; C) displays the CI; D) displays the fraction of neurons out of all cells in the network; E) displays the length of axons. The boxplot representations of data from each culture are displayed and colored according to treatment with PMA, GOE or neither.

These are the results of an unpaired single-sample student's t-test. Data collected from CC2. Asterisks denote statistical significance, one for $p < 0.05$, two for $p < 0.01$ and three for $p < 0.001$. Outliers are marked by crosses.

4 Discussion

4.1 Prototype Review

The optogenetic stimulation platforms are the centerpieces of this work. These stimulators were easy to handle – they were robust and sturdy. When placed in the incubator, they were relatively stable – due to the weight placed inside, the force required to displace the stimulators was sufficient to withstand the light handling experienced during medium exchange. An exception arose when it came to the ribbon cable connections. These need to be handled very carefully. When closing the lid, the ribbon cable became bent and at times disconnected from the circuit. This only arose when opening and closing the lid, however, which would not be done during a stimulation session. However, such a problem could be solved by simply soldering the connection.

The intensity of the LEDs remained constant over the LTS experiment. However, during the first, unsuccessful experiment, the intensity of S1's LEDs subsided. This was solved by adding jumper cables between the microcontroller and ribbon cable, as stated previously. Intensity did not subside after this change was made. While line flashing, the phenomenon that causes LEDs to illuminate slightly when not intentionally triggered, was observed in S1 due to its circuitry being setup for matrix multiplexing, it is unclear whether this had a measurably different effect on CC1 than CC2, which was stimulated by S2.

Cellular medium needed to be changed twice a week; it was important that the cell carriers be placed in the exact same positions as before. This was relatively simple, as the cell carrier and carrier interface had the same asymmetric shape. One simply needed to match these when returning the cell carrier to the stimulator. Minor shifts < 2 mm can be ignored due to the homogenous stimulation approach implemented in this work.

Regarding the results of the temperature and humidity test: As the temperature was the same as the rest of the incubator, this is evidence that the LED array did not produce enough heat to potentially disturb neuronal cell cultures. However, the humidity did increase slightly. As this is a minor increase, it may be negligible. However, as these measurements were taken approximately 24 h apart, humidity may become more of a factor when stimulating for longer periods. Nonetheless, after the week-long LTS experiment, no significant humidity increase was observed visually in the stimulators.

Both prototypes were capable of interfacing with the standardized 12-well cell culture carriers, and each well's LED was individually controllable by changing settings in a configuration file.

For future versions, it might be interesting to be able to vary the height between LED and cell culture.

4.2 Explanatory Models for LTS Experiment Results

What exactly happens to cortical tissue under intense and continuous optogenetic stimulation remains an open question. Understanding the effects of new technologies is the key to leveraging their advantages while mitigating their disadvantages. Like continuous electrical stimulation, one would expect long-term optogenetic stimulation to have substantial consequences for network development. One of our hypotheses is that excessively strong long-term stimulation would be ultimately detrimental and lead to cell death, as well as impacts on neuronal migration. This is backed up by previous experiments, which are discussed in later sections (Marek et al. 2019; Moulin et al. 2019; Yoshifumi Abe et al. 2019; Köhidi et al. 2017).

However, we must also consider the role that transfection plays in the health of neuronal networks. Transfection via viral vectors can induce lower neuron density by impairing metabolism (Detrait et al. 2002). As all cultures are transfected by the same method, they will ideally all be the same before stimulation.

4.2.1 Impact of LTS on Cell Survival

Optogenetic stimulation can affect cell health in two main ways: excitotoxicity and phototoxicity. Phototoxicity occurs when fluorescent molecules are illuminated. These react with molecular oxygen, producing free radicals, which can damage organelles and other cellular components (Nikon's MicroscopyU 2023). Phototoxic effects therefore directly disrupt metabolic processes which can lead to cell death. During experiments wherein neuronal networks were exposed to wavelengths of light ≤ 480 nm, phototoxic reactions were observed (Marek et al. 2019). Due to this phototoxicity, neurons may enter apoptosis or simply suffer necrosis. However, phototoxic effects lead to more than just cell death among neurons. Glial cells would also be affected, as would the axons and dendrites between neurons.

The underlying mechanism of excitotoxicity involves intracellular acidification via Ca^{2+} (Maimon et al. 2018). This approach assumes successful transfection of enough neurons in the network to express ChR2, such that the network can be functionally stimulated by the experimentation platform's LEDs. When ChR2 is stimulated excessively, large amounts of intracellular Ca^{2+} are released. According to models of homeostatic neurite growth, such an influx could also impair axon length as well as the motility of their growth cones (Okujeni 2012; van Ooyen et al. 1995).

In another experiment, motor control neurons were optogenetically stimulated long-term, resulting in motor dysfunction and a reduction in the diameters of neuronal dendrites and axons (Yoshifumi Abe et al. 2019). Such a reduction in diameter would lead to slower AP propagation (Egert, Okujeni 2022). Similarly, mice with optogenetically treated hippocampus CA1 pyramidal neurons were stimulated for 24 h with 15 ms pulses of blue light every 90 s (Moulin et al. 2019). In the CA1 region, dendritic spine densities and areas were reduced compared to controls. Chronic stimulation also impaired the induction of long-term potentiation and facilitated that of long-term depression in CA1. This would weaken postsynaptic responses (Egert, Okujeni 2020). These are two examples of phototoxic and/or excitotoxic effects caused by optogenetic LTS.

Interestingly, CC1 and CC2 had in some cases wildly differing results for the same stimulation frequencies. For example, CC1's neuron density among GOE cultures decreased as stimulation frequency increased while PMA cultures first increased, then decreased in density with increasing stimulation frequency. In turn, CC2's neuron densities remained largely constant over all stimulation frequencies. Such differing results might also be indicative of differences between the two stimulators. Namely, line flashing might come in to play here, as the extra stimulation between set LED pulses might have more strongly impacted neuronal densities. However, the possibility that the neuronal densities of some of CC1's cultures decreased because of an excitotoxic or phototoxic effect cannot be ruled out. However, this model does not explain why neuronal densities in control cultures and CC2 did not decrease.

Another explanation we must consider is that the stimulation was not effective. This could have been due to the CaMKII promoter not being upregulated in younger cell cultures, leading to a lower expression of ChR2. However, this would be inconsistent with previous findings which showed that optogenetic stimulation of ChR2 expressing neurons under regulation of the CaMKII promoter during early network growth was a detriment to neuronal migration (Köhidi et al. 2017). Another possibility is that a lack of sufficient ChR2 expression may be attributed to the short expression period prior to the beginning of the LTS experiment and overall very low CHR2 expression and impact of stimulation. However, a longer initial

expression period prior to stimulation could have likewise resulted in little impact on neuronal migration and neurite outgrowth due to structural maturity already having been attained (Okujeni and Egert 2019). In such a case, no obvious influence on the degree of clustering would be expected.

4.2.2 Impact of LTS on neuronal migration

Concerning migration of neurons and their subsequent clustering, stark differences were observed between cell culture groups. Neuronal migration and clustering crucially impact network connectivity, modularity and activity dynamics (Okujeni and Egert 2019). The impact of LTS on this process could therefore depend on baseline migration rates. These can be modulated by PKC manipulation (Okujeni 2012). To test this, we stimulated networks with differently modulated PKC activity via chronic exposure to PKC agonists or antagonists. The overall impact of PKC manipulation on the developing network structure was only partially consistent with previous reports (Okujeni et al. 2017; Okujeni and Egert 2019). PMA treated cultures were more strongly clustered that controls and GOE treated cultures. However, we could not detect any difference in clustering between GOE treated cultures and controls, which may be due to the low number of networks analyzed.

Interestingly, all cultures were roughly in the same range of the clustering index. This could be explained by the same mechanism which decreased cell migration in (Köhidi et al. 2017), namely, cell motility being impaired by optogenetic stimulation. This reduces the cells' effective migrative range, meaning that neurons cannot travel as far to create large clusters. What we would see are more homogenous networks. Indeed, according to the results, many networks are more homogenous compared to previous reports (Okujeni and Egert 2019). This model does not explain why the same high CI of all three cultures is also seen for no stimulation. Again, this could be due to the low number of cultures studied.

As stimulation was started at 6 DIV, migration and clustering (which take up until 1-2 WIV to complete (Okujeni and Egert 2019)) may or may not have been completed before ChR2 had been sufficiently expressed. ChR2's promoter, CaMKII, is upregulated only after these processes are complete. This leads to the conclusion that migration and clustering wouldn't be impacted by optogenetic stimulation. This is contrary to previous in vitro findings (Köhidi et al. 2017).

4.2.3 Impact of LTS on axon growth

What we would expect to see after optogenetic LTS is reduced neurite growth. However, we also expect reductions in neuron density and clustering. This could be explained by a compensatory neurite growth, because as neuron density decreases, neurons become further apart from each other, and so axons and dendrites must extend further to reach other neurons (Okujeni and Egert 2019).

The results show that high neuron density is reflected by shorter axons, and vice versa. These changes in axon length can be explained by the homeostatic regulation of neurite growth in conjunction with the observed changes in neuron density (Okujeni and Egert 2019).

4.2.4 Summary of Findings

We have found slight evidence for detrimental effects of optogenetic long-term stimulation. Namely, decreases in neuronal densities and clustering are definitive signs for such adverse effects. Neurite growth may also be impaired; however, results show that these effects are overpowered by the homeostatic regulation of neurite growth as neuron densities decrease. Further speculation is cut short by largely inconclusive data.

4.3 Effectiveness of Optogenetic Stimulation

In order to determine whether or not the LEDs were capable of stimulating neuronal networks at the distance present between LED and cell culture in the stimulators, stimulation experiments were performed on cultures grown on MEAs which had been transfected for 15 days.

Recorded signal profiles clearly depict action potentials and network bursts. As these signal recordings are all timed with the flashing of the LED, it suggests that these neuron firings were the result of successful optogenetic stimulation. Moreover, we found that neuronal responses consist of an early response, most likely directly induced action potentials, as well as a late response consisting of recurrent polysynaptic network activation. Such signals are indicative of induced network bursts. Photoelectric effects come into play here too, as light can knock electrons in a metal into the conduction band, producing an electric current. The metal in question here would be the electrodes. The photoelectric effect can indeed be observed in the

recorded MEA data; however, artefacts of this nature are simple to differentiate from true neuronal signals. Some electrodes supplied noisy data of varying amplitudes. This is most likely due to wear and tear of the MEAs, which can be recycled for up to 300 DIV of service.

Concerning CC4 and CC5, only photoelectric effects could be observed. As these cultures were younger than CC3, it is possible that ChR2 had not yet been expressed within the 3 DIV expression time before the experiment to make the neuronal network sufficiently sensitive to light.

The findings of these MEA experiments show that the LED used for the stimulators can successfully stimulate optogenetically treated neuronal networks. Importantly, the distance from LED to the network (6 mm) is sufficiently close to stimulate the network. This is the same distance between LED and cell culture as in the stimulators. Therefore, this is evidence that the stimulators are capable of optogenetic stimulation of neuronal networks, assuming such networks express enough ChR2.

4.4 Relevance of Results

These findings, in particular the slight evidence for optogenetic stimulation-induced decreases in cell viability, will have consequences for the field of optogenetics. Research with more cell cultures should be conducted in order to acquire better, more accurate data. Studies could be made into the effects of stimulation at lower frequencies (≤ 0.1 Hz). The existence of this platform offers optogeneticists a useful tool to further study long-term optogenetic stimulation.

As only 2 cultures were successfully stimulated, an optimal minimum of $n = 3$ experiments was not reached.

5 Summary

In summary, we successfully developed an optogenetic stimulation platform, constructed two prototypes and performed long-term stimulation experiments with them. Due to the MEA results, we concluded that the distance between LED and cell culture is sufficiently small such that stimulation could occur. Results of LTS experiments were largely inconclusive; we believe this to be mostly attributed to the short expression time of ChR2, as well as the small sample size. However, slight evidence for detrimental effects of optogenetic LTS was observed. In particular, decreases in cell motility and density were discovered. Tentative evidence for promotion of neurite growth was found, however, we believe this to largely be the effects of homeostatic regulation of neurite outgrowth as neuron densities decrease.

This platform has the potential for conducting further research, as well as further iteration. In particular, giving biologists more tools for their research will increase the pace of progress in this field. Novel biomedical implants such as cochlear implants may be developed with optogenetic technology, as well as new neuronal therapies for patients with brain injuries. For these types of applications, it is especially important to study possible morphogenic changes brought about by optogenetic LTS. Optogenetics is a burgeoning field with many possibilities; the work done in this study strives to aid researchers in developing this technology.

6 Acknowledgments

This bachelor's thesis is the result of many weeks of hard work, which would have been impossible to complete without the help and support of the many kind people around me and those that I have met through this work.

First of all, my heartfelt gratitude goes to my supervisor Dr. Samora Okujeni, who, thanks to his constant support and advice, guided me through the many pitfalls of working in a primarily biological regime as an engineer. His knowledge in the fields of neuroscience, optogenetics and biology in general helped me orient myself in an unfamiliar environment.

My thanks also go out to Prof. Dr. Ulrich Egert, who assigned me this project and always gave clear advice. His input was instrumental to the development of the stimulation platform.

I am especially grateful to Ute Boltze, who was always ready to help in the lab and without whom I would not have had as much fun.

My sincere thanks also go to the rest in Professor Egert's group; Esther Flores, Patricia Cseh and Gundel Jäger. Thank you all for making me feel so welcome at IMTEK.

Last but not least, my unending gratitude goes out to my friends and family. Your constant love and support carried me through this process. Without your comments and advice, this thesis would have been a lot messier.

7 Bibliography

Detrait, Eric R.; Bowers, William J.; Halterman, Marc W.; Giuliano, Rita E.; Bennice, Lisa; Federoff, Howard J.; Richfield, Eric K. (2002): Reporter gene transfer induces apoptosis in primary cortical neurons. In *Molecular therapy : the journal of the American Society of Gene Therapy* 5 (6), pp. 723–730. DOI: 10.1006/mthe.2002.0609.

Egert, Ulrich; Okujeni, Samora (2020): Neuroscience for Engineers. Freiburg im Breisgau. PDF.

Egert, Ulrich; Okujeni, Samora (2022): Biology for Engineers. PDF.

Ghassaei, Amanda (2012): Arduino Timer Interrupts. Instructables. Available online at https://www.instructables.com/Arduino-Timer-Interrupts/, updated on 7/8/2012, checked on 1/31/2023.

Keppeler, Daniel; Schwaerzle, Michael; Harczos, Tamas; Jablonski, Lukasz; Dieter, Alexander; Wolf, Bettina et al. (2020): Multichannel optogenetic stimulation of the auditory pathway using microfabricated LED cochlear implants in rodents. In *Science translational medicine* 12 (553). DOI: 10.1126/scitranslmed.abb8086.

Köhidi, Tímea; Jády, Attila G.; Markó, Károly; Papp, Noémi; Andrási, Tibor; Környei, Zsuzsanna; Madarász, Emília (2017): Differentiation-Dependent Motility-Responses of Developing Neural Progenitors to Optogenetic Stimulation. In *Frontiers in cellular neuroscience* 11, p. 401. DOI: 10.3389/fncel.2017.00401.

Lambert de Rouvroit, C.; Goffinet, A. M. (2001): Neuronal migration. In *Mechanisms of development* 105 (1-2), pp. 47–56. DOI: 10.1016/s0925-4773(01)00396-3.

Lignani, Gabriele; Ferrea, Enrico; Difato, Francesco; Amarù, Jessica; Ferroni, Eleonora; Lugarà, Eleonora et al. (2013): Long-term optical stimulation of channelrhodopsin-expressing neurons to study network plasticity. In *Frontiers in molecular neuroscience* 6, p. 22. DOI: 10.3389/fnmol.2013.00022.

Lin, John Y. (2011): A user's guide to channelrhodopsin variants: features, limitations and future developments. In *Experimental physiology* 96 (1), pp. 19–25. DOI: 10.1113/expphysiol.2009.051961.

Maeda, E.; Robinson, H. P.; Kawana, A. (1995): The mechanisms of generation and propagation of synchronized bursting in developing networks of cortical neurons. In *The Journal of Neuroscience* 15 (10), pp. 6834–6845. DOI: 10.1523/JNEUROSCI.15-10-06834.1995.

Maimon, Benjamin E.; Diaz, Maurizio; Revol, Emilie C. M.; Schneider, Alexis M.; Leaker, Ben; Varela, Claudia E. et al. (2018): Optogenetic Peripheral Nerve Immunogenicity. In *Scientific reports* 8 (1), p. 14076. DOI: 10.1038/s41598-018-32075-0.

Marek, V.; Potey, A.; Réaux-Le-Goazigo, A.; Reboussin, E.; Charbonnier, A.; Villette, T. et al. (2019): Blue light exposure in vitro causes toxicity to trigeminal neurons and glia through increased superoxide and hydrogen peroxide generation. In *Free radical biology & medicine* 131, pp. 27–39. DOI: 10.1016/j.freeradbiomed.2018.11.029.

Max Jürgen Wechlin (2022): Entwicklung eines LED-Arrays zur optogenetischen Stimulation von neuronalen Netzwerken in vitro. Bachelor. Albert-Ludwigs-Universität, Freiburg im Breisgau. IMTEK.

McAlinden, Niall; Massoubre, David; Richardson, Elliot; Gu, Erdan; Sakata, Shuzo; Dawson, Martin D.; Mathieson, Keith (2013): Thermal and optical characterization of micro-LED probes for in vivo optogenetic neural stimulation. In *Optics letters* 38 (6), pp. 992–994. DOI: 10.1364/OL.38.000992.

Moulin, Thiago C.; Petiz, Lyvia L.; Rayêe, Danielle; Winne, Jessica; Maia, Roberto G.; Da Cruz, Rafael V. Lima et al. (2019): Chronic in vivo optogenetic stimulation modulates neuronal excitability, spine morphology and Hebbian plasticity in the mouse hippocampus. In *Hippocampus*. DOI: 10.1101/320507.

Nagel, Georg; Ollig, Doris; Fuhrmann, Markus; Kateriya, Suneel; Musti, Anna Maria; Bamberg, Ernst; Hegemann, Peter (2002): Channelrhodopsin-1: a light-gated proton channel in green algae. In *Science (New York, N.Y.)* 296 (5577), pp. 2395–2398. DOI: 10.1126/science.1072068.

Nichia Corporation (2022): Specifications for UV LED NSPU510CS. Datasheet.

Nikon's MicroscopyU (2023): Phototoxicity in Microscopy Literature References. Available online at https://www.microscopyu.com/references/cellular-phototoxicity, updated on 1/14/2023, checked on 1/14/2023.

Okujeni, Samora (2012): Coevolution of structure and activity dynamics in self-organizing networks of cortical neurons. Inauguraldissertation zur Erlangung der Doktorwürde. PhD. Albert-Ludwigs-Universität, Freiburg im Breisgau. Fakultät für Biologie.

Okujeni, Samora; Egert, Ulrich (2019): Self-organization of modular network architecture by activity-dependent neuronal migration and outgrowth. In *eLife*. Available online at DOI: https://doi.org/10.7554/eLife.47996.

Okujeni, Samora; Kandler, Steffen; Egert, Ulrich (2017): Mesoscale Architecture Shapes Initiation and Richness of Spontaneous Network Activity. In *The Journal of Neuroscience* 37 (14), pp. 3972–3987. DOI: 10.1523/JNEUROSCI.2552-16.2017.

Oliver Paul (2020): Skript zur Vorlesung Halbleiterphysik. Albert-Ludwigs-Universität.

Paschotta, Rüdiger (2022): Optical Intensity. RP Photonics AG. Available online at https://www.rp-photonics.com/optical_intensity.html, updated on 1/31/2023, checked on 1/31/2023.

Ramakers, G. J.; Corner, M. A.; Habets, A. M. (1990): Development in the absence of spontaneous bioelectric activity results in increased stereotyped burst firing in cultures of dissociated cerebral cortex. In *Experimental brain research* 79 (1), pp. 157–166. DOI: 10.1007/BF00228885.

Reddy, Jay W.; Kimukin, Ibrahim; Stewart, Luke T.; Ahmed, Zabir; Barth, Alison L.; Towe, Elias; Chamanzar, Maysamreza (2019): High Density, Double-Sided, Flexible Optoelectronic Neural Probes With Embedded μLEDs. In *Frontiers in neuroscience* 13, p. 745. DOI: 10.3389/fnins.2019.00745.

Steriade, Mircea; Timofeev, Igor (2003): Neuronal plasticity in thalamocortical networks during sleep and waking oscillations. In *Neuron* 37 (4), pp. 563–576. DOI: 10.1016/S0896-6273(03)00065-5.

Stevens, C. F.; Zador, A. M. (1998): Input synchrony and the irregular firing of cortical neurons. In *Nature neuroscience* 1 (3), pp. 210–217. DOI: 10.1038/659.

Tennant, Kelly A.; Taylor, Stephanie L.; White, Emily R.; Brown, Craig E. (2017): Optogenetic rewiring of thalamocortical circuits to restore function in the stroke injured brain. In *Nature Communications* 8 (1), p. 15879. DOI: 10.1038/ncomms15879.

Valley, Matthew; Wagner, Sebastian; Gallarda, Benjamin W.; Lledo, Pierre-Marie (2011): Using affordable LED arrays for photo-stimulation of neurons. In *Journal of visualized experiments : JoVE* (57). DOI: 10.3791/3379.

van Ooyen, A.; van Pelt, J.; Corner, M. A. (1995): Implications of activity dependent neurite outgrowth for neuronal morphology and network development. In *Journal of theoretical biology* 172 (1), pp. 63–82. DOI: 10.1006/jtbi.1995.0005.

van Pelt, Jaap; Vajda, Ildiko; Wolters, Pieter S.; Corner, Michael A.; Ramakers, Ger J. A. (2005): Dynamics and plasticity in developing neuronal networks in vitro. In *Progress in brain research* 147, pp. 173–188. DOI: 10.1016/S0079-6123(04)47013-7.

Weisstein, Eric W. (2023): Spherical Cone. From MathWorld - A Wolfram Web Resource. Available online at https://mathworld.wolfram.com/SphericalCone.html, updated on 1/31/2023, checked on 1/31/2023.

Yoshifumi Abe; Yuji Komaki; Fumiko Seki; Shinsuke Shibata; Hideyuki Okano; Kenji F. Tanaka (2019): Correlative study using structural MRI and super-resolution microscopy to detect structural alterations induced by long-term optogenetic stimulation of striatal medium spiny neurons. In *Neurochemistry International* Volume 125, Article ISSN 0197-0186, Pages 163–174.